NUMERICAL ANALYSIS
OF
FILM COOLING

by
Ömer TAŞTEKİN
B.S. in M.E., B.Ü., 1983

Submitted to the Faculty of Engineering
in Partial Fulfillment of the Requirements
for the Degree of

MASTER OF SCIENCE
in
Mechanical Engineering

Boğaziçi University
January, 1983

APPROVED BY

Doç.Dr.Muhsin Mengütürk

Mechanical Engineering Department (Advisor)

Doç.Dr.Fahir Borak

Chemical Engineering Department

Dr.Vahan Kalenderoğlu

Mechanical Engineering Department

ACKNOWLEDGEMENTS

I would like to express my gratitude to my thesis supervisor, Doç.Dr.Muhsin Mengütürk, for his constructive suggestions and helpful discussions.

ABSTRACT

A numerical model is developed to investigate film cooling in compressible laminar boundary layer flows. This model is applied to the first stage stator blade of a transonic gas turbine. As a prelude study, film cooling for incompressible flow over a flat plate is also included. Film cooling effectiveness is reported for a variety of injection configurations so that the effects of coolant mass flow rate, injection angle, and slot width can be investigated. For the coolant mass flow rates considered, normal injection provides better cooling than inclined injection. However, normal injection brings about greater boundary layer thickness and may reduce aerodynamic performance. Use of multiple slots provides higher and more uniform effectiveness for the s me coolant mass flow rate.

ÖZET

Laminer sınır tabakalı akışlarda film soğutma olayını incelemek için nümerik bir model geliştirilmektedir. Bu model transonik bir gaz türbininin birinci kademe stator kanatlarının soğutulmasını incelemek için kullanılmaktadır. Ön çalışma olarak bir düzlemin film soğutma problemi de ele alınmaktadır. Soğutucu kütle debisinin, injeksiyon açısının, 'slot' genişliğinin soğutma etkenliği üzerindeki etkisi araştırılmaktadır. Aynı soğutucu kütle debisi için, normal injeksiyon eğik ve teğetsel injeksiyondan daha etken olmaktadır. Ancak normal injeksiyon daha büyük sınır tabaka kalınlıklarına yol açmakta ve aerodinamik performansı düşürmektedir. Birden fazla injeksiyon 'slot'ının kullanılması soğutma etkenliğini büyük ölçüde artırmaktadır.

TABLE OF CONTENTS

LIST OF FIGURES

LIST OF TABLES

LIST OF SYMBOLS

Symbol	
u, v	Velocity components
T	Temperature
p	Pressure
ρ	Density
μ	Viscosity
x	Longitidunal coordinate
y	Transverse coordinate
c	Reference length (chord)
Re	Reynolds number, $(\rho_o U_o c)/\mu_o$
Pr	Prandtl number, $(\mu_o C_p)/k_o$
E	Eckert number, $U_o^2/(C_p(T_o-T_c))$
C_p	Specific heat at constant pressure
M	Mach number, $U/\sqrt{\gamma RT}$
η	Film cooling effectiveness
F	Blowing rate parameter
$\dot{M}_c$	Coolant mass flow rate
s	Slot width
x_o	Slot leading edge distance
α	Injection angle
L	Distance between slots
$\bar{x}$, $\bar{y}$	Dimensionless coordinates x/c, y/c
$\bar{u}$, $\bar{v}$ or U, V	Dimensionless velocity u/U_o, v/U_o
$\bar{T}$	Dimensionless temperature, $(T-T_c)/(T_o-T_c)$
$\bar{p}$	Dimensionless pressure, $p/\rho_o U_o^2$
$\bar{\mu}$	Dimensionless viscosity, μ/μ_o
$\bar{\rho}$	Dimensionless density, ρ/ρ_o
ϕ	Viscous dissipation
k	Magnification factor
N	Step size number in transverse direction
ϵ	Error bound

Subscripts

r	Recovery
aw	Adiabatic wall with injection
c	Coolant
os	Reference stagnation
e	Outer edge
o	Free stream reference
x	Local
n	Nodal point in transverse direction
m	Station number in streamwise direction

Superscripts

-	Dimensionless
a	Assumed
c	Computed

CHAPTER I

INTRODUCTION

Methods for shielding a solid surface exposed to a high temperature gas stream are of considerable interest. Among them, film cooling is considered to be the most promising and is used in many engineering applications such as cooling of rocket nozzles, reentering space vehicles, and gas turbine blades. This study is concerned with film cooling of stator blades of a gas turbine.

Film cooling analysis reported in this study is restricted to two dimensional laminar compressible flow with slot injection and is achieved by solving boundary layer equations numerically employing finite difference method. Both mainstream and coolant are air. As a preliminary work, film cooling for incompressible flow over a flat plate is considered. Then film cooling problem of a gas turbine stator blade is examined in detail (The term 'film cooling problem' will signify the problem of determining the effects of physical and geometrical parameters of film cooling on film cooling effectiveness).

Film cooling is a process to protect solid surfaces exposed to high temperature environment, which, in general is gaseous. It is of great importance and used in many engineering applications such as cooling of rocket nozzles, gas turbine blades, and reentering space vehicles. In this method, a secondary fluid called coolant is injected from one or more discrete locations (slots or holes) along the surface exposed to high temperature effect into the boundary layer developing on the surface. The secondary fluid serves two functions: 1) The introduction of coolant which is at a temperature lower than the mainstream into the boundary layer reduces the temperature in the region downstream of injection region, 2) Injection of coolant increases the boundary layer thickness. Increased boundary layer thickness, in turn, tends to decrease the heat transfer to the wall.

The geometry and flow field at the point of injection are significant variables in film cooling. In two dimensional film cooling, both the external flow and the secondary fluid are introduced uniformly across the span as in Fig.1. Secondary fluid can enter through a porous region (Fig.1.a) or through a continuous slot at some angle to the wall surface and mainstream (Fig 1.b and 1.c).

Although three dimensional film cooling is outside the scope of the present work, it will be briefly discussed due to its practical importance. In three dimensional film cooling, the injection of secondary fluid is not uniform across the span, but rather occurs at isolated locations often through discrete holes in the surface (Fig.2). This can lead to the jets of secondary fluid being blown off the surface and the mainstream flow coming between or under the coolant jets decreasing the effectiveness of film cooling process. Even so, for structural reasons, when it is difficult to have a truly-continuous two dimensional injection slot, interrupted slots and rows of multiple slots have been used (Fig.2).

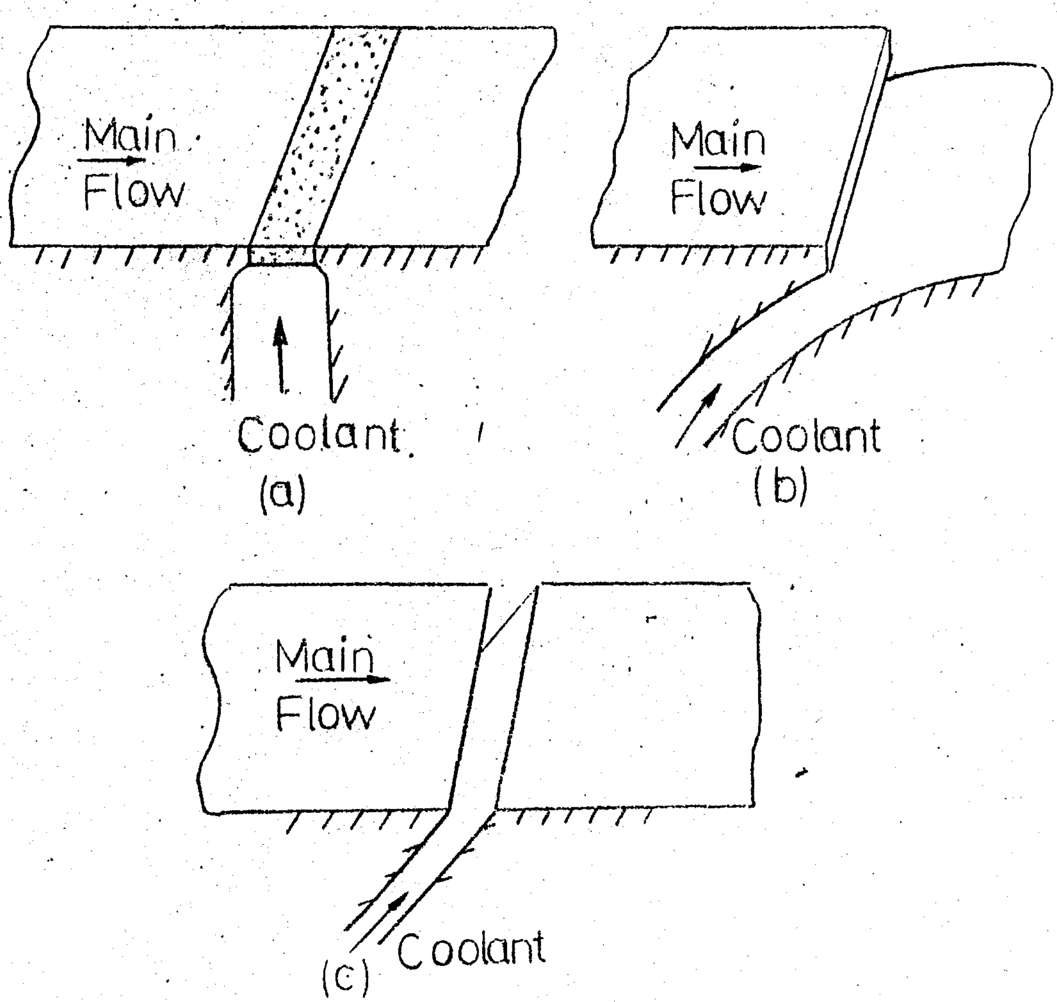

Fig.1- Film cooling geometry for two dimensional film cooling

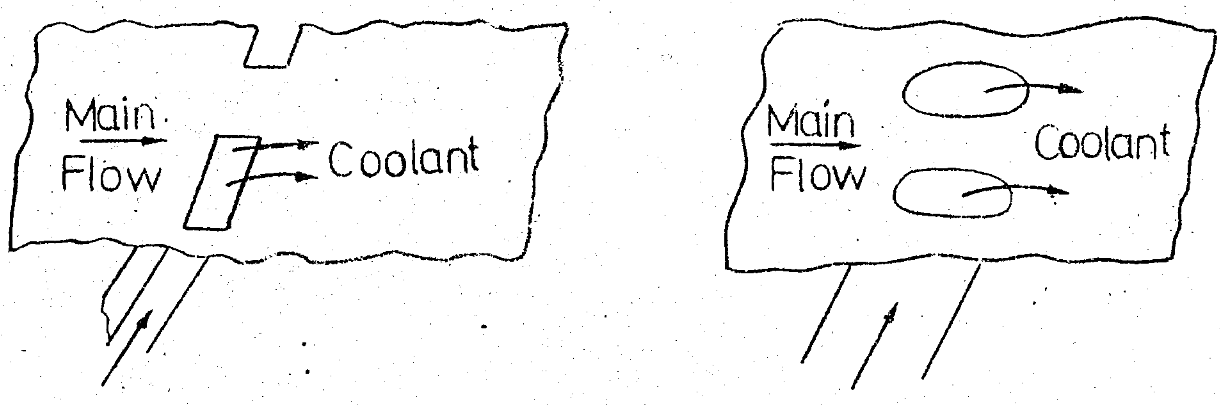

Fig.2- Three dimensional film cooling geometry

Film cooling effectiveness is a major parameter in determining how well the injection flow shields the wall from the mainstream gas. In general, it is defined as

$$\eta = \frac{T_r - T_{aw}}{T_r - T_c} \tag{I.1}$$

where

T_r is recovery temperature (i.e., adiabatic wall temperature evaluated in the absence of coolant)

T_{aw} is adiabatic wall temperature with injection

T_c is coolant temperature

If the flow is essentially subsonic as in the present case, the following formula can be used:

$$\eta = \frac{T_{os} - T_{aw}}{T_{os} - T_c} \tag{I.2}$$

where, T_{os} is the reference stagnation temperature which remains constant outside the boundary layer (Note that in low speed flows, viscous dissipation is not so important, thus $T_r \approx T_{os}$. However, in high speed flows, this is not valid and the first formula is to be utilized). Furthermore, if there is no pressure gradient (i.e., $T_e = T_o$ = const.), it can be replaced by

$$\eta = \frac{T_o - T_{aw}}{T_o - T_c} \qquad (I.3)$$

where, T_o denotes reference free stream static temperature, T_e stands for outer edge static temperature. The last definition is especially suitable and common to film cooling for incompressible flow over a flat plate.

The use of T_{aw} in the definitions is meaningful. In film cooling applications, the heat transfer from the hot gas to the surface to be protected is not zero. There is usually some type of internal cooling, but the limiting case (i.e., the highest wall temperature) is adiabatic wall. In addition, it is used as reference temperature in evaluation of convection conductance in high speed heat convection.

Note that film cooling effectiveness varies from unity at the point of injection, where $T_{aw} \approx T_c$, to zero far downstream of the slot, where, because of dilution of the coolant, the adiabatic wall temperature approaches the free stream stagnation temperature.

Significant geometrical and physical parameters in film cooling are:

Blowing rate parameter $F=\rho_c v_c/\rho_o U_o$ or

$F=v_c/U_o$

Coolant mass flow rate	$\dot{M}_c = \rho_c v_c s$
Slot width	s
Starting length	x_o
Injection angle	α
Distance between consecutive slots	L
Free stream reference values	U_o, T_o, p_o (or ρ_o)

In these definitions, U_o stands for reference free stream velocity, v_c for normal component of injection velocity ρ_o for reference free stream density, ρ_c for coolant density, T_o for reference free stream static temperature, and p_o for reference free stream static pressure.

For the present work, film cooling geometry is illustrated in Fig.3.

In the following sections, Chap.II reviews previous work on two dimensional film cooling. Chap.III, presents theoretical formulation and describes numerical method. In Chap.IV, the results obtained from numerical analysis are discussed. In Chap.V, following a brief summary, the findings of the present study are given. Finally, details of numerical formulation is provided in Appendix.

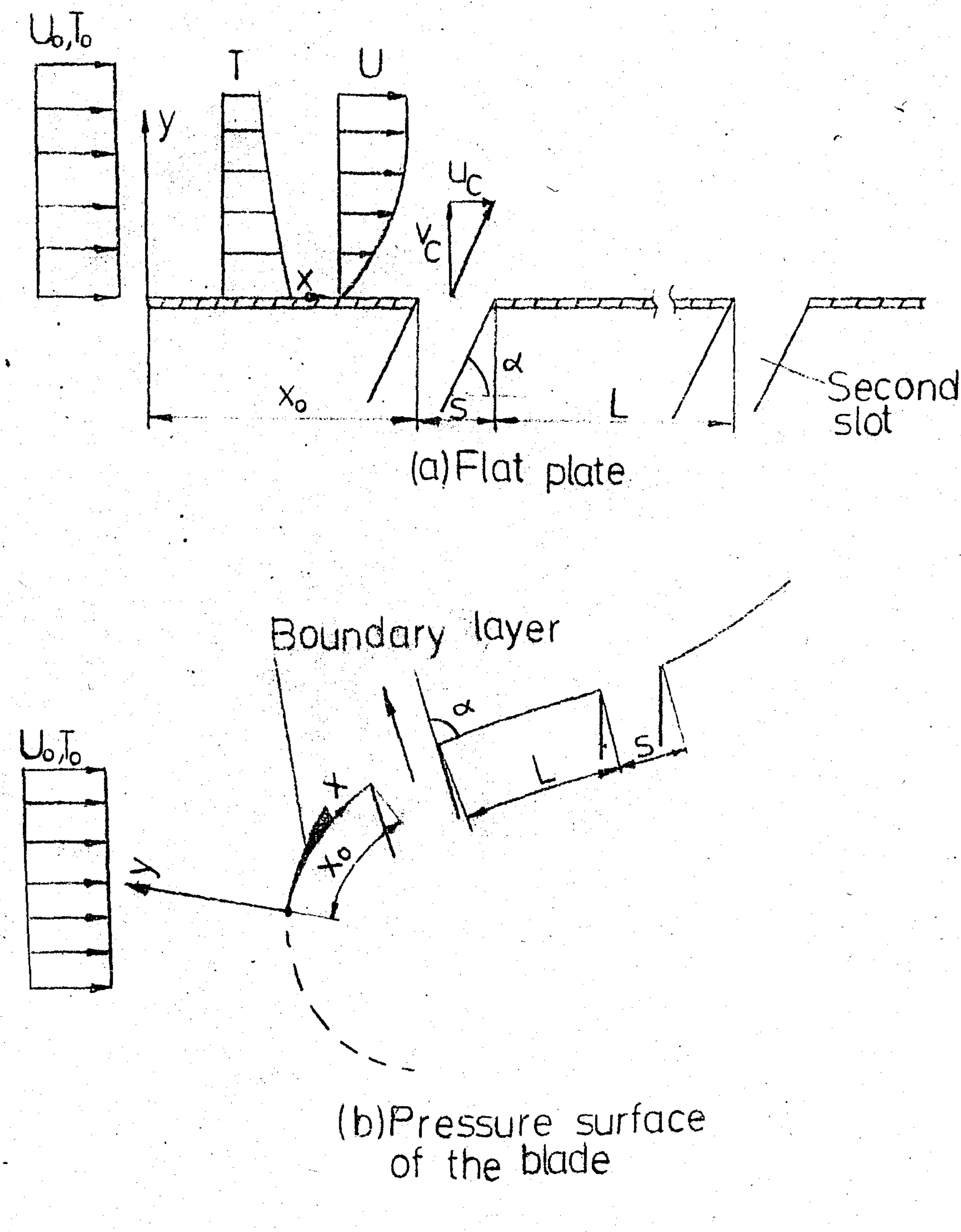

Fig.3- Injection geometry for the present study

CHAPTER II

PREVIOUS WORK ON TWO DIMENSIONAL FILM COOLING

There are different approaches to handle film cooling process. One of them is heat-sink model. In this theory, hydrodynamic effect of injected fluid is completely neglected for sufficiently low injection rates, which is justified only far downstream of the slot. As a result, use of turbulent boundary layer properties is made possible (e.g., 1/7 power law velocity profile). With the aid of boundary layer integral analysis and turbulent flow characteristics, film cooling effectiveness is obtained as(1)

$$\eta = C \left(\frac{X}{F's}\right)^{-0.8} \qquad \text{(II.1)}$$

where, C is, in general, a complicated function of slot Reynolds number, $Re_s = (u_c s)/\nu_c$, blowing rate parameter (or injection ratio), $F' = \rho_c u_c/\rho_o U_o$ and slot geometry, and lies between 15 and 25 according to the various experimental studies(2). In these definitions, u_c stands for tangential component of injection velocity, ν_c for coolant kinematic viscosity, and X for the distance measured from the trailing edge of slot.

There are numerous experiments parallel to this theory.

In these studies, effectiveness determined experimentally is fitted to the form obtained analytically. Hartnett et all(1), obtained velocity, temperature distributions, effectiveness, and heat transfer coefficient for air injected through a tangential slot into a turbulent boundary layer. They used a single injection rate (F'=0.28), a fixed mainstream velocity and a single slot size. The injection geometry is shown in Fig.4.

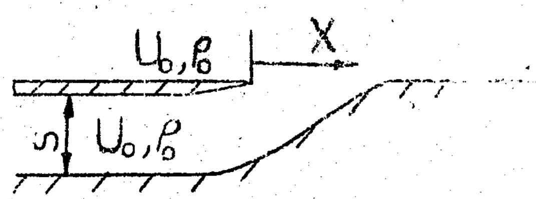

Fig.4- Injection geometry for the study of Hartnett et all(1)

In that study, the following correlation was found by semi-empirical analysis as:

$$\eta = 16.9 \left(\frac{X}{F's}\right)^{-0.8} , \quad \frac{X}{F's} \geq 60 \qquad \text{(II.2)}$$

Seban(3) studied heat transfer and effectiveness for a turbulent boundary layer with tangential fluid injection. Experiments are reported to be conducted for different slot sizes and injection ratios for the geometry illustrated in Fig.5.

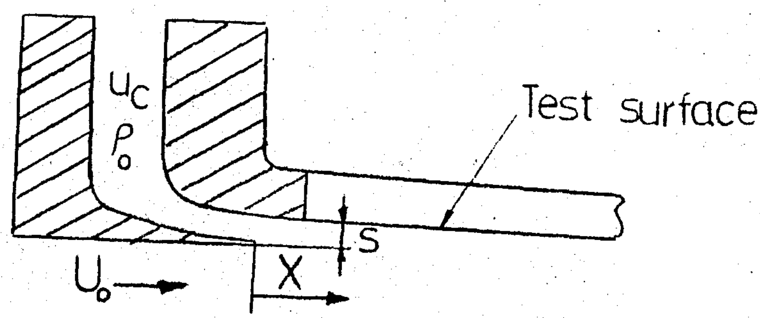

Fig.5- Slot geometry in Seban's study(3)

Correlations were obtained for $F' \lessgtr 1$. The most suitable correlation is given to be

$$\eta = 25(F')^{1.2} \left(\frac{X}{s}\right)^{-0.8} \quad , F' < 0.9 \tag{II.3}$$

For $F' > 1$ a correlation was also achieved (not given here due to its lengthy). It is reported that for $F' > 1$ effectiveness is reduced as injection rate increases; however, it is always greater than that obtained for $F' = 0.6$. Haering (2), investigated the effect of the mainfold width on the effectiveness for various injection rates less than unity (Fig.6).

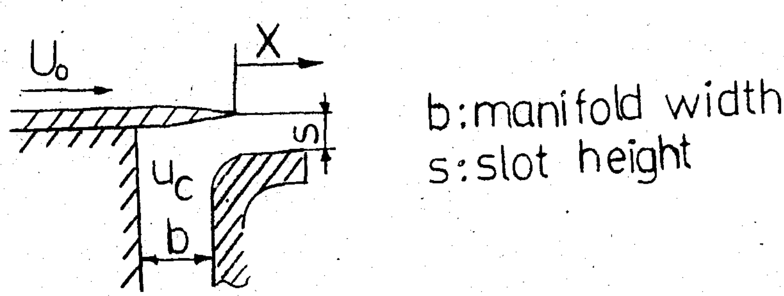

Fig.6- Geometry in the study of Haering(2)

It is noted that for F' < 0.5 manifold width effect can be neglected. For 1 > F'> 0.5, larger manifold widths yield greater effectiveness. The correlation coefficient, C is given as 17. Goldstein et all(4) considered the case where coolant is injected through a porous section into a turbulent free stream (Fig.7).

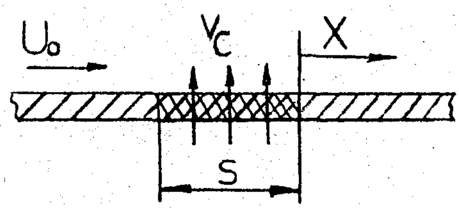

Fig.7- Injection geometry for the study of Goldstein et all(4)

Effectiveness was determined for various values of coolant temperature, blowing rate, and free stream velocity. The correlation is given as:

$$= C(\frac{X}{Fs})^{-0.88} \qquad (II.4)$$

where, $21.5 \leq C \leq 24.5$

From the comparisons with the earlier, experimental studies, it was concluded that, using a porous wall for film cooling for protection of a surface would produce similar effect to that obtained for injection through a nearly tangential slot, and that small differences in detail arose from the differences in slot geometry. Seban and Back(5), studied effectiveness for a turbulent boundary layer with tangential injection and variable free stream velocity (Fig.5). The free stream velocity was increased from 1.6 to 2.4 times along the plate length. The effectiveness turned out to be only slightly below the values which would have existed if the free stream velocity had remained at its original value.

Spalding(6) reviewed earlier correlations given by various experimenters for the cases $F' \gtrless 1$ and noted that there were similarities between these correlations. As a result, an artificially contrived formula which would fit all of the data is proposed as:

$$
\begin{aligned}
&= 1 \quad \text{for} \quad \bar{X} < 7 \\
&= 7/\bar{X} \quad \text{for} \quad \bar{X} \geq 7
\end{aligned}
\qquad \text{(II.5)}
$$

where,

$$\bar{X} = 0.91\left(\frac{U_o X}{u_c s}\right) Re_s^{-0.2} + \{\left|1.41 \quad 1 - \frac{U_o}{u_c}\right| \frac{X}{s}\}^{0.5}$$

This correlation agrees satisfactorily with the data of most experimenters. This and similar models are exhaustively discussed in an article by Goldstein(7). In these studies, analytical and experimental results agree well downstream of injection region where the hydrodynamic effect of the injected fluid is trivial. This method suffers from the inaccuracy near the injection region because the hydrodynamic effect of injected fluid is neglected and turbulent boundary layer characteristics are used as if there were no injection.

Mayle and Kopper(8), present a similar analytical model for turbulent boundary layer with tangential slot injection. This model accounts for separate development of the thermal boundary layer (In the first model discussed, it is implicitly assumed that the thermal and hydrodynamic boundary layers have the same thickness). Using turbulent boundary layer exuations and turbulent flow properties, effectiveness was determined in terms of the ratio between the two boundary layer thicknesses, $\delta h/\delta t$. It was concluded that the streamwise decay in effectiveness might be explained by considering the thermal boundary layer growth within the hydrodynamic boundary layer. This model is not successful in explaining the flow behaviour in the immediate vicinity of the injection region, either.

More recently, numerical methods have been used. Boundary layer equations are solved numerically. Usually finite difference method is used. Spalding(9), studies tangential injection into a turbulent boundary layer over flat plate and into confined ducts. Effects of Mach number, coolant Reynolds number, coolant temperature and injection ratio, u_c/U_o are presented. In addition, foreign gas injection (i.e., mass transfer) is taken into account. Nilson and Tsuei(10,11) consider laminar oblique injection into low and high speed compressible flow past over a flat plate and discuss the effects of blowing rate parameter, slot spacing, injection angle, free stream Mach number, and multiple slots. Inger and Swean(12), provide a similarity solution to vectored injection into laminar boundary layers with zero pressure gradient for a wide range of injection rates. They account for heat transfer as well. However, their solution is restricted to continuous injection (i.e., porous wall or many slots closely spaced) and is not applicable to discrete slot injection.

CHAPTER III

A N A L Y S I S

III.1. GOVERNING EXUATIONS AND BOUNDARY CONDITIONS

The flow in a steady two dimensional laminar compressible boundary layer is described by the following set of partial differential equations:

Continuity:

$$\frac{\partial}{\partial \bar{x}}(\bar{\rho}\bar{u}) + \frac{\partial}{\partial \bar{y}}(\bar{\rho}\bar{v}) = 0 \qquad \text{(III.1.1)}$$

Momentum:

$$\bar{\rho}\bar{u}\frac{\partial \bar{u}}{\partial \bar{x}} + \bar{\rho}\bar{v}\frac{\partial \bar{u}}{\partial \bar{y}} = -\frac{d\bar{p}}{d\bar{x}} + \frac{1}{Re}\frac{\partial}{\partial \bar{y}}\left(\bar{\mu}\frac{\partial \bar{u}}{\partial \bar{y}}\right) \qquad \text{(III.1.2)}$$

Energy:

$$\bar{\rho}\bar{u}\frac{\partial \bar{T}}{\partial \bar{x}} + \bar{\rho}\bar{v}\frac{\partial \bar{T}}{\partial \bar{y}} = E\bar{u}\frac{d\bar{p}}{d\bar{x}} + \frac{1}{Re}\frac{\partial}{\partial \bar{y}}\left(\frac{\bar{\mu}}{Pr}\frac{\partial \bar{T}}{\partial \bar{y}}\right) + \frac{E}{Re}\frac{\bar{\mu}}{\bar{\rho}}\left(\frac{\partial \bar{u}}{\partial \bar{y}}\right)^2 \qquad \text{(III.1.3)}$$

where,

$\bar{x},\bar{y}$ dimensionles coordinates $\bar{x} = x/c$, $\bar{y} = y/c$

$\bar{u},\bar{v}$ dimensionles velocity components $\bar{u}=u/u_o$ $\bar{v}=v/u_o$

$\bar{T}$ dimensionles temperature $\bar{T} = (T-T)/(T_o-T_c)$

$\bar{p}$ dimensionles pressure $\bar{p} = p/\rho_o U_o^2$

$\bar{\rho}$ dimensionles density $\bar{\rho} = \rho/\rho_o$

$\bar{\mu}$ dimensionles viscosity $\bar{\mu} = \mu/\mu_o$

Re reference Reynolds number $Re = \rho_o U_o C/\mu_o$

Pr reference Prandtl number $Pr = \mu_o C_p/k_o$

E Eckert number $E = U_o^2/C_p(T_o-T_c)$

Due to large temperature differences $\bar{\mu} = \bar{\mu}(\bar{T})$, $\bar{\rho} = \bar{\rho}(\bar{p},\bar{T})$. As complementary equations. Sutherland's viscosity formula and equation of state are used

$$\frac{\mu}{\mu_o} = \left(\frac{T}{T_o}\right)^{3/2} \frac{T_o + S}{T + S} \tag{III.1.4}$$

$$\rho = P/RT \tag{III.1.5}$$

For air, $S = 110^oK$. Cebeci,T and Smith,A.M.O.(13) yield $Pr = Pr(T)$ distribution, which is used in the present formulation (Note that air is assumed to be perfect gas).

The above equations are used, in general. For incompressible flow over a flat plate, it suffices to take $Pr(\bar{T}) = Pr$, $\bar{\mu} = \bar{\rho} = 1$, and $\frac{dp}{d\bar{x}} = 0$.

The boundary layer equations are subject to the following boundary conditions:

Impervious and adiabatic wall ($\bar{x}\leq\bar{x}_o$ and $\bar{x}>\bar{x}_o+\bar{s}$)

$$\text{At } \bar{y} = 0 \qquad \begin{aligned} \bar{u} &= 0 \\ \bar{v} &= 0 \\ \frac{\partial \bar{T}}{\partial \bar{y}} &= 0 \end{aligned} \qquad \text{(III.1.6)}$$

Slot conditions $(\bar{x}_o + \bar{s} \geq \bar{x} > \bar{x}_o)$

$$\text{At } \bar{y} = 0 \qquad \begin{aligned} \bar{U} &= (\rho_o U_o F/\rho_c)\cot\alpha = \bar{u}_c \\ \bar{v} &= (\rho_o U_o F)/\rho_c = \bar{v}_c \\ \bar{T} &= 0 \end{aligned} \qquad \text{(III.1.7)}$$

Outer edge conditions (For all $\bar{x}$'s)

$$y \to \infty \qquad \begin{aligned} \bar{u} &= \bar{U}_e(\bar{x}) \\ \bar{T} &= \bar{T}_e(\bar{x}) \end{aligned} \quad \text{or} \quad \begin{aligned} \bar{u} &= 1 \\ \bar{T} &= 1 \end{aligned} \qquad \text{(III.1.8)}$$

Compressible Incompressible

Once velocity field has been established, outer edge conditions are calculated as follows:

$$T_e = T_{os} - \frac{U_e^2}{2C_p} = T_o + \frac{1}{2C_p}(U_o^2 - U_e^2) \qquad \text{(III.1.9)}$$

$$P_e = P_o \left(\frac{T_e}{T_o}\right)^{\gamma/(\gamma-1)} \qquad \text{(III.1.10)}$$

where, γ is ratio of specific heats, C_p is specific heat at constant pressure (Note that since the outer flow is inviscid and adiabatic, total enthalpy or stagnation temperature remains outside the boundary layer. Moreover, since outer flow is potential isentropic relations can be employed).

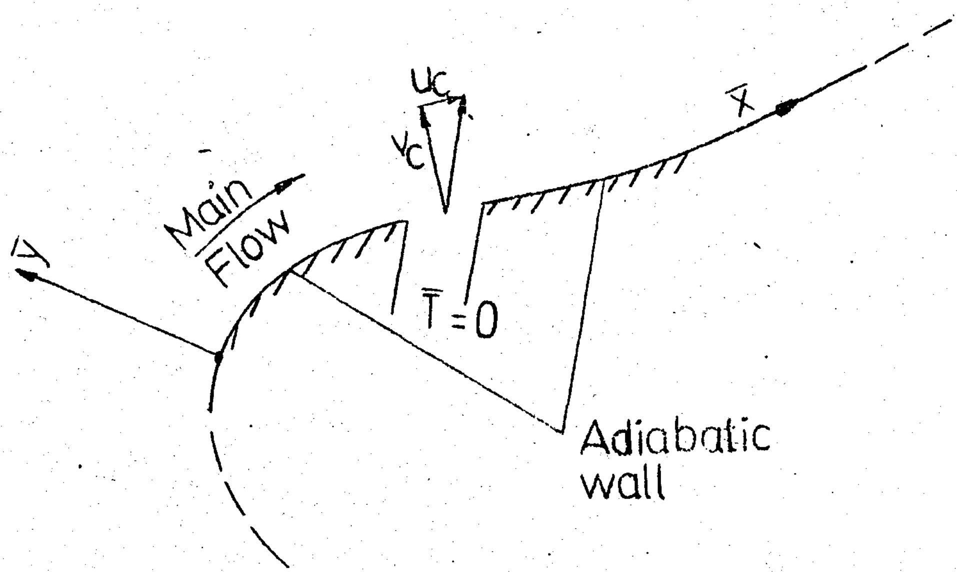

Fig.8- Boundary conditions and injection geometry

It should be noted that normal component of injection velocity must be small enough so as not to violate boundary layer assumptions. Otherwise, inviscid free stream flow may be disturbed; furthermore, boundary layer may be blown off the wall (i.e., separation of boundary layer). In this case, classical boundary layer equations are no longer valid. Then, how large an injection rate can be applied. In general, it is required that

$$\frac{v_c}{U_o} \sqrt{Re_x} = 0(1) \qquad \text{(III.1.11)}$$

where

$$Re_x = \frac{\rho_e U_e x}{\mu_e}$$

The above requirement is not strict and given for continuous injection(14,15). Rather crude criterion is provided by Wallace and Kemp(16) as

$$\frac{v_c}{U_o} < 0.1 \qquad \text{(III.1.12)}$$

Eckert(17) gives the blow-off limit for incompressible flow over flat plate with uniform injection as

$$\frac{v_c}{U_o} \sqrt{Re_x} = 0.619 \qquad \text{(III.1.13)}$$

It is seen that the above criteria are related to continuous injection. For slot injection, it is proposed in this study that

$$\frac{v_c}{U_o} \sqrt{Re^*} = 0(1) \qquad \text{(III.1.14)}$$

where,

$$Re^* = \frac{\rho_e U_e s}{\mu_e}$$

This criterion proved to agree with the present injection study and yields upper limit. On the other hand, $Re^* = \frac{\rho_e U_e x_o}{\mu_e}$ is more conservative.

In case of accelerated flows, injection velocity can take higher values because of favourable pressure gradient effect (As known, injection produces unfavourable pressure gradient effect on the flow, which can be balanced by accelerating the flow). Eckert(17) yields the blow-off limit as 3.191 for plane stagnation flow with uniform injection (for flat plate, 0.619). Thus, in accelaretad flows larger injection rates can be applicable. In what follows, some references regarding the studies for large injection rates are cited.

Wallace and Kemp(16), propose an analytical model for uniform injection at large rates. It is assumed that boundary layer equations cease to be valid. Instead, three layer model is adopted. 1) Inviscid rotational layer near the surface 2) Shear layer 3) Incident flow. Results are obtained for wedge and plane stagnation flows.

For compressible wedge flow with uniform injection, there are numerical studies(18,19,20,21) based on the assumption that boundary layer equations are still valid. Their analysis is restricted to pressure coefficient $\beta = 0.5$.

Nilson and Tsuei(10,11) apply large injection velocities for compressible flow over a flat plate with slot injection. They report that they use revised form of Patankar-Spalding method to solve boundary layer equations and also report that their formulation and grid system is extremely suitable to severe injection rates.

In the present study, the numerical formulation developed is restricted to the injection rates allowable by previously-mentioned criteria. In other words, large injection rates cannot be attained by the present formulation.

III.2. NUMERICAL METHOD

An implicit finite difference scheme is employed to solve the boundary layer equations. The computational grid used in formulation is illustrated in Fig.9. In streamwise direction, both constant and variable step sizes are adopted. Variable step size is used downstream of the slot to reduce computational time. In transverse direction, variable step size is used to control local truncation error as well as to reduce computational time. Transverse coordinates are computed as

$$\bar{y}_n = \Delta\bar{y}_o \frac{k^{n-1} - 1}{k - 1} \qquad n=2,\ldots,N \qquad \text{(III.2.1)}$$

where, k stands for magnification factor, N for maximum step number in transverse direction, $\Delta\bar{y}_o$ for initial step size

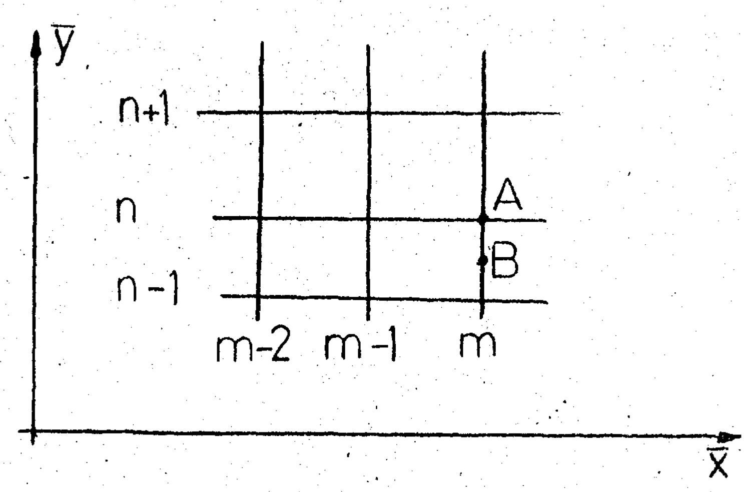

Fig.9- Computational grid

For the partial derivatives in $\bar{x}$-direction, three-point difference scheme is employed due to the parabolic nature of the equations. However, at first stations downstream of the slot ends, simple backward difference formulation is used due to discontinuity existing at slot ends. Partial derivatives in $\bar{y}$-direction are centered about point A (Fig.9) due to the elliptic nature of the equations in this direction. The continuity equation is centered about point B (Fig.9). Except for the backward difference, other schemes are accurate to the second order.

The numerical formulation developed necessitates two upstream tangential velocity and temperature profiles, which are obtained by running Cebeci's computer program(22). The outer edge velocity distribution for flow over the blade is obtained from Katsanis' program(23). For incompressible flow over flat plate, the outer edge velocity is constant and the velocity distribution prior to the injection slot is given by the Blasius' solution(24).

Boundary layer equations for compressible flow are coupled since viscosity, density, and Pr number are functions of temperature. In incompressible flow, however, there is no coupling between the equations, and only momentum equation is non-linear. In what follows, the procedure followed is described mainly for compressible flow. Derivation of finite difference equations and details of the method are given in the appendix.

Since, as noted earlier, field equations are non-linear a simple iterative procedure is employed. In dervinig difference equations, velocity and temperature profiles at the present station are assumed to be known. Thus, density, viscosity and Pr number can be computed from the assumed temperature profile. Once derivatives have been approximated by previously-mentioned schemes, momentum and energy equations take the forms

$$\begin{aligned} B_n \bar{u}_{n+1} + C_n \bar{u}_n + D_n u_{n-1} &= E_n \\ \bar{B}_n \bar{T}_{n+1} + \bar{C}_n \bar{T}_n + \bar{D}_n \bar{T}_{n-1} &= \bar{E}_n \end{aligned} \qquad \text{(III.2.2)}$$

where, $\bar{u}_n$, $\bar{T}_n$ are dimensionless velocity and temperature values at each nodal point of the present station. Coefficients are calculated from the first two initial velocity and temperature profiles and from assumed profiles. It can readily be noted that both equations can be formed into three-block diagonal matrix equations, which are solved by the Gaussian elimination method modified for three-block diagonal matrices. First, the difference form of the momentum equation is solved with suitable boundary conditions. Once the tangential velocity component at each grid point of the present station has been obtained, the difference form of the continuity equation is solved and the normal velocity component distribution is determined. Then, the difference form of the energy equation is solved in a similar way. Computed values of the tangential and normal component of velocity and temperature are assigned as assumed profiles.

Density, viscosity and Pr number are recomputed with this new assumed temperature profile. Using the new coefficients, the difference equations are solved again and the whole procedure is repeated until the desired accuracy is attained (Here, iteration is carried out over tangential component of velocity. See Appendix). The values computed at each station are used as initial guess for the solution at the next station. In the case of incompressible flow, iterations are performed only for the momentum and continuity equation. Once the velocity distribution has been established, the energy equation is solved directly (Recall that the energy equation is linear).

The accuracy of the numerical formulation has been tested for the following cases 1) Incompressible flow over flat plate (Blasius solution): Test runs were performed for different Re numbers and grid spacings. Fig.10 shows that the results of the present study agree with the Blasius solution very well. 2) Compressible flow over the pressure surface of the stator blade a) with impervious and adiabatic wall b) with uniform injection where the coolant is at a substantially lower temperature than the free strem temperature. The results are compared with the velocity and temperature profiles obtained from Cebeci's computer program(22). Again, as can be noted in Fig.11 and 12, the agreement is quite good. In these cases, relative error in tangential velocity and temperature profiles is less than 0.2 % 3) Incompressible flow over a flat plate with slot suction: This case was included to test the accuracy of the formulation for discontinuous boundary condition. The skin friction coefficient distribution over and downstream of the slot obtained from the present study compares very well with the result of Nilson and Tsuei(11) as indicated in Fig.13.

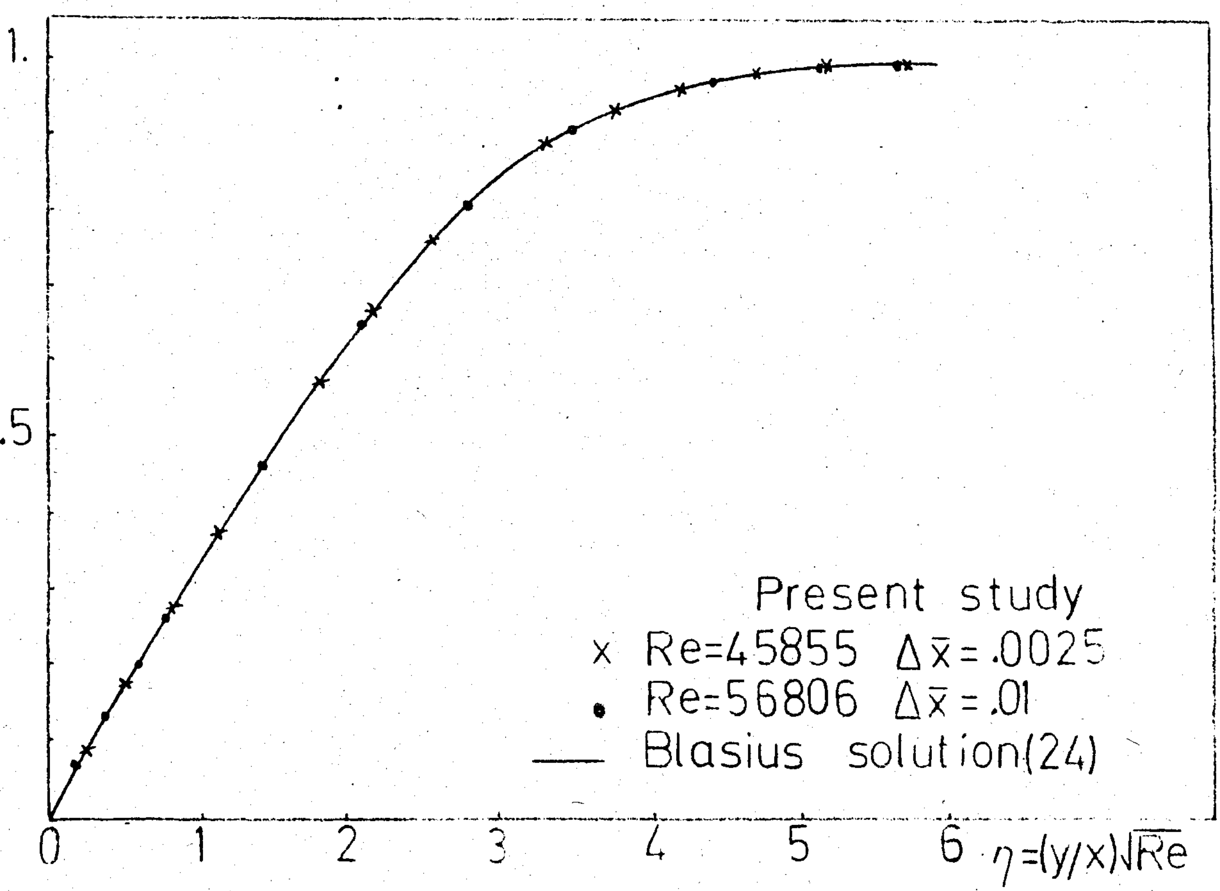

Fig.10- Comparison of the present formulation with the Blasius' solution(24)

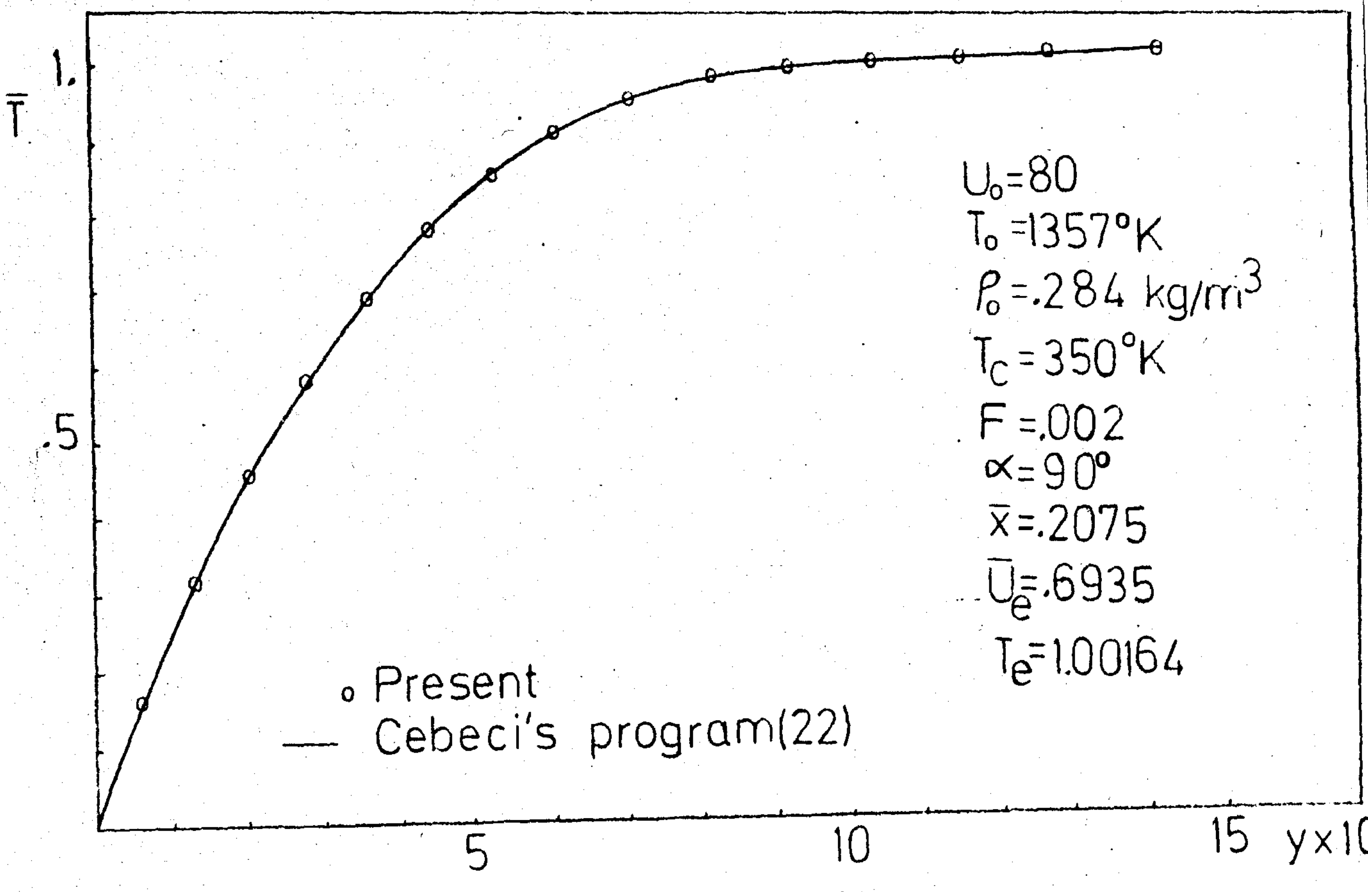

Fig.11- Comparison of the present work with the results obtained from Cebeci's program(22) for uniform injection

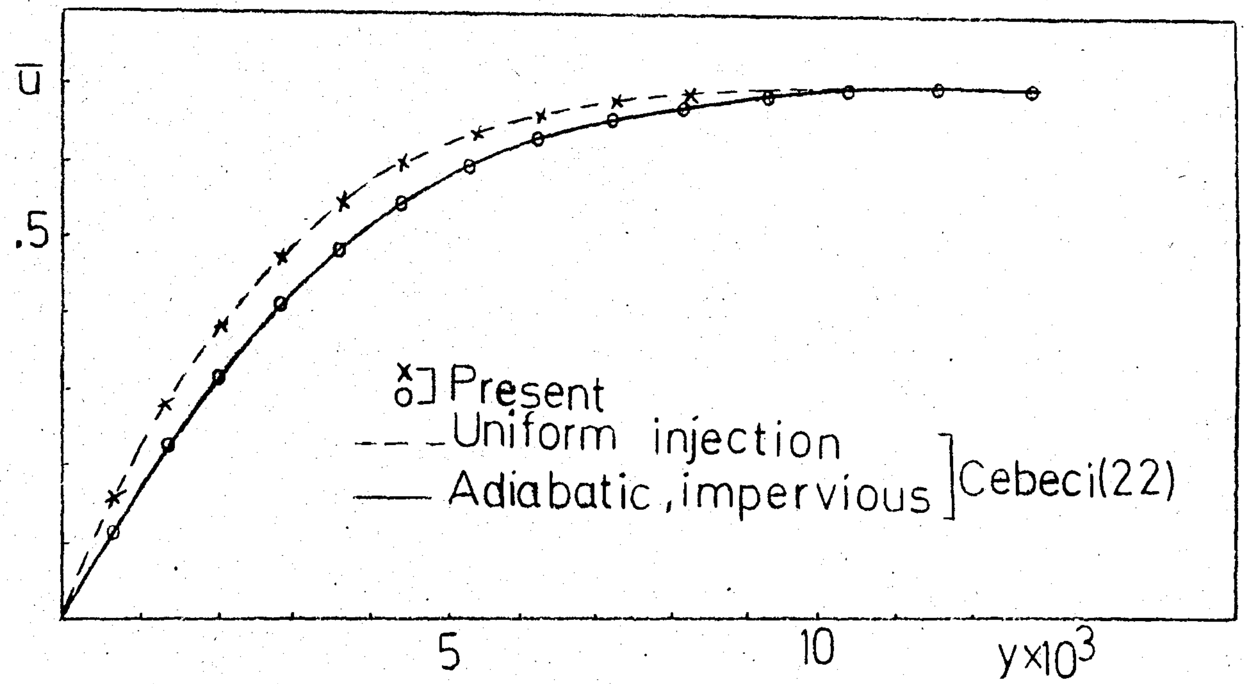

Fig.12- Comparison of the present study with the results of Cebeci's computer program(22) for uniform injection and adiabatic, impervious wall

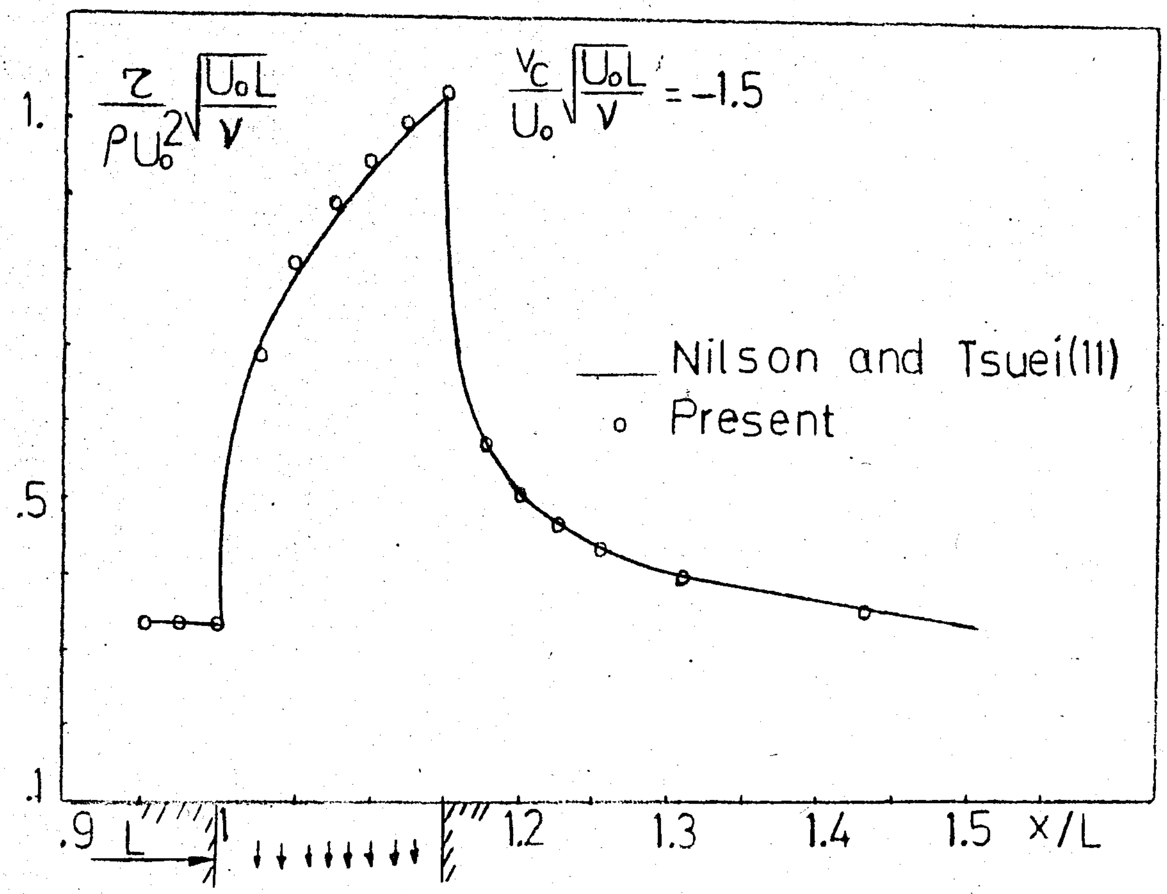

Fig.13- Comparison of skin friction coefficient for slot suction

CHAPTER IV
RESULTS AND DISCUSSION

IV.1. FILM COOLING BY OBLIQUE SLOT INJECTION FOR INCOMPRESSIBLE FLOW OVER A FLAT PLATE

As a preliminary study, incompressible film cooling by oblique slot injection has been investigated. Characteristic length, free stream velocity and temperature difference have been taken as 10 cm, 20 m/s and $50^\circ C$, respectively. (Note that temperature difference and free stream velocity have been so chosen that the incompressible assumption is not violated. Free stream Mach number, $M_o = 0.0416$). Effects of coolant mass flow rate, $\dot{M}_c = \rho_c v_c S$, injection angle and slot width have been investigated. In general, injection angle varies between 0° and 90°. It can be assumed that the range, $0^\circ < \alpha < 15^\circ$ would correspond to tangential injection, $15^\circ < \alpha < 75^\circ$ to inclined injection, $75^\circ < \alpha < 90^\circ$ to normal injection. Throughout the present study, injection angles of 6°, 45°, and 84° have been used to characterize tangential, inclined, and normal injection, respectively. Two different slot widths (S = 0.16 cm and 0.32 cm) have been considered. Although the incompressible flow over flat plate is of little practical importance, this analysis is useful in observing trends and in making comparisons. Fig.14 shows typical velocity profiles at the trailing edge of slot for tangential, inclined and normal injection.

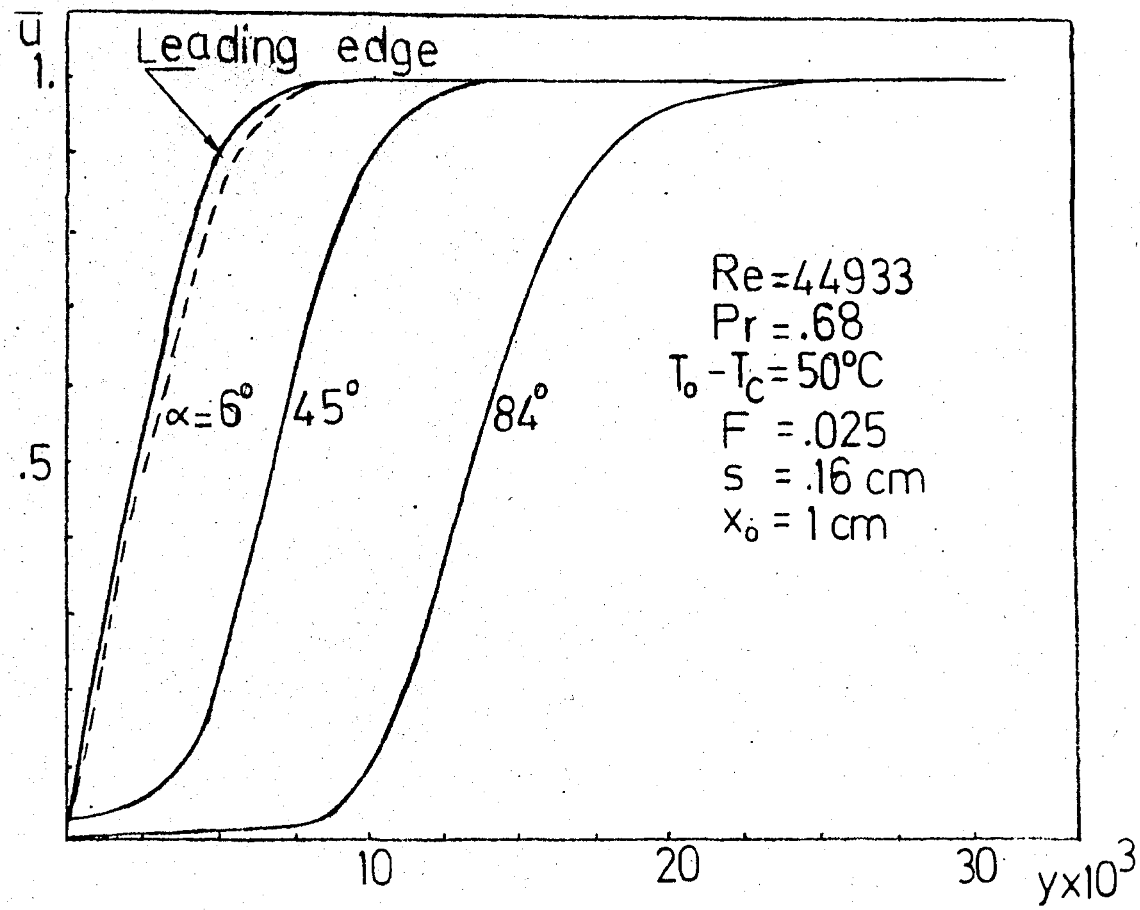

Fig.14- Velocity profiles at the trailing edge of the slot for different injection angles.

As expected, maximum boundary layer thickness is attained in the case of normal injection. Fig.15 and Fig.16 show effectiveness for normal, inclined and tangential injection. The effect of the slot width have been studied by holding the coolant mass flow rate fixed and is shown in Fig.17.

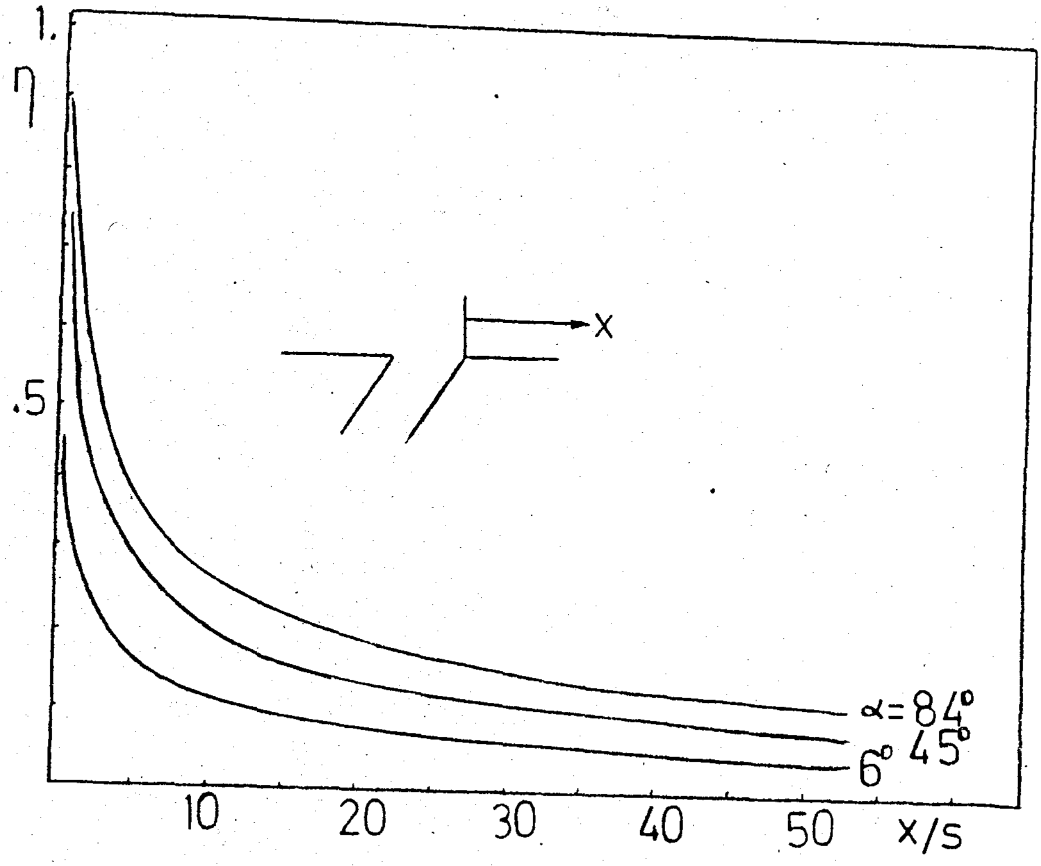

Fig.15- Comparison of effectiveness for different injection angles

Film cooling is realized by a combination of two basic effects a) increase in boundary layer thickness that reduces the rate of heat transfer, and b) Mixing of coolant and main-stream gas that directly reduces the temperature of the latter. The boundary layer thickness increases, as the injection angle increases. Therefore, at large injection rates maximum effectiveness is obtained in the case of normal injection (Fig.15). At low injection rates, the first effect is negligible and mixing is the dominant cooling mechanism. Consequently, the effect of injection angle on cooling decreases as the injection rate is reduced (Fig.16).

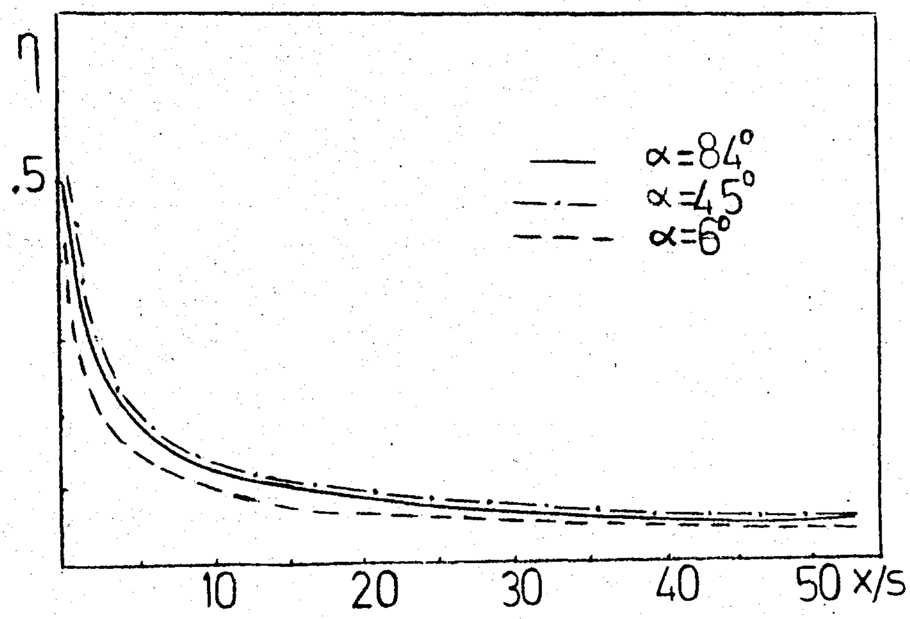

Fig.16- Effect of injection angle at low injection rates.

The dominant cooling mechanism for tangential and inclined injection is the mixing effect. Wide slot provides better mixing of coolant and mainstream gas. Therefore, wide slot is more effective for inclined and tangential injection (Fig.17). This is more pronounced for tangential injection. However, boundary layer thickness effect (i.e., insulation effect) dominates over the mixing effect for normal injection. Use of wide slot reduces injection velocity, thus causing thinner boundary layer thickness. Hence, narrow slot is more effective for normal injection (Fig.17). Similar results are reported by Nilson and Tsuei(10).

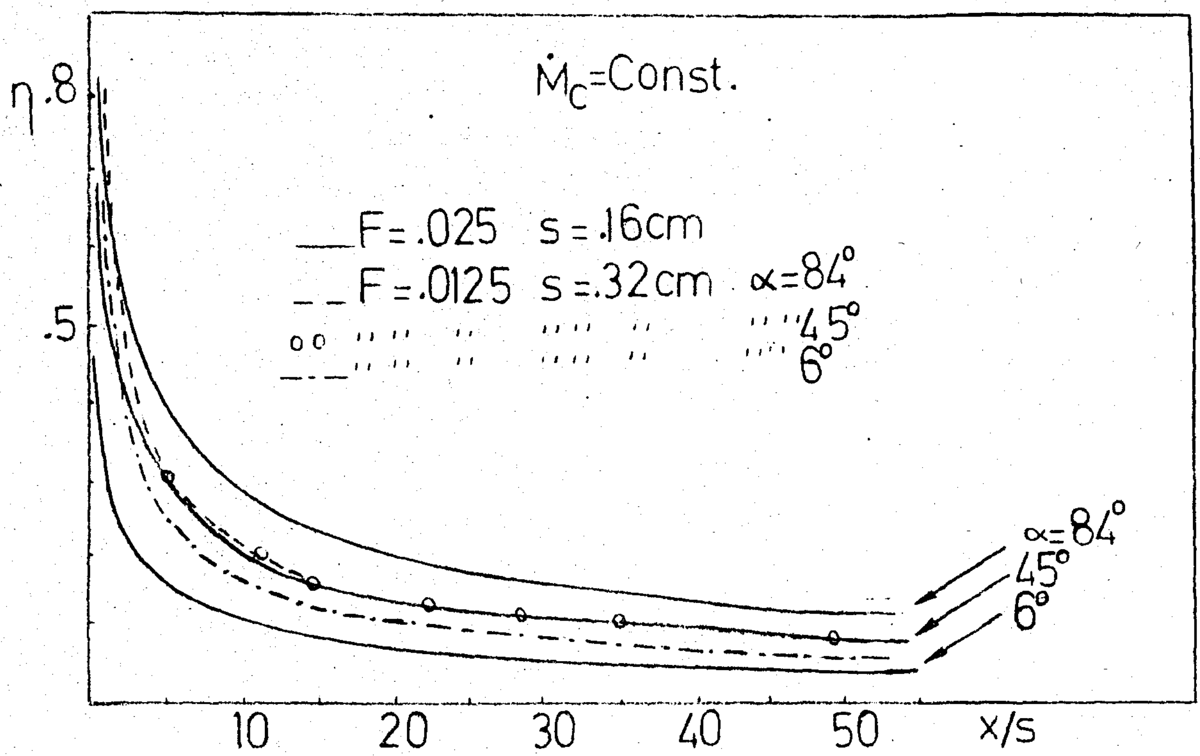

Fig.17- Effect of slot width for different injection angles.

IV.2. FILM COOLING OF FIRST STAGE STATOR SECTION BLADE OF A GAS TURBINE

In this section, film cooling of the first stage stator of a large transonic gas turbine is considered. Results have been obtained by solving the boundary layer equations with the imposed pressure gradient. Fig.18 shows the blade profile and the flow pattern around it. The numerical application considered here is restricted to the pressure surface of the blade, since injection from suction surface would cause separation. Besides, accelerated flow over the pressure surface causes thinner boundary layer (i.e., poor insulation). Therefore, film cooling of the pressure surface is more interesting. Furthermore, due to structural reasons and strength considerations, tangential injection is not suitable for turbine blade cooling and has been excluded.

Free stream reference conditions (just outside the blade section) have been chosen as To = 1357^{o}K, Po = 1.12×10^{5} N/m^{2}. The values of film cooling parameters used in this study and the corresponding cases studied are presented in Table 1.

Fig.19 shows the outer edge velocity and temperature distributions obtained from Katsanis(23) program for the two different free stream velocity or Mach numbers (Mo = 0.135 and 0.27) as a function of the surface length. Origin of the coordinate system is the leading edge stagnation point predicted by Katsanis' program(23).

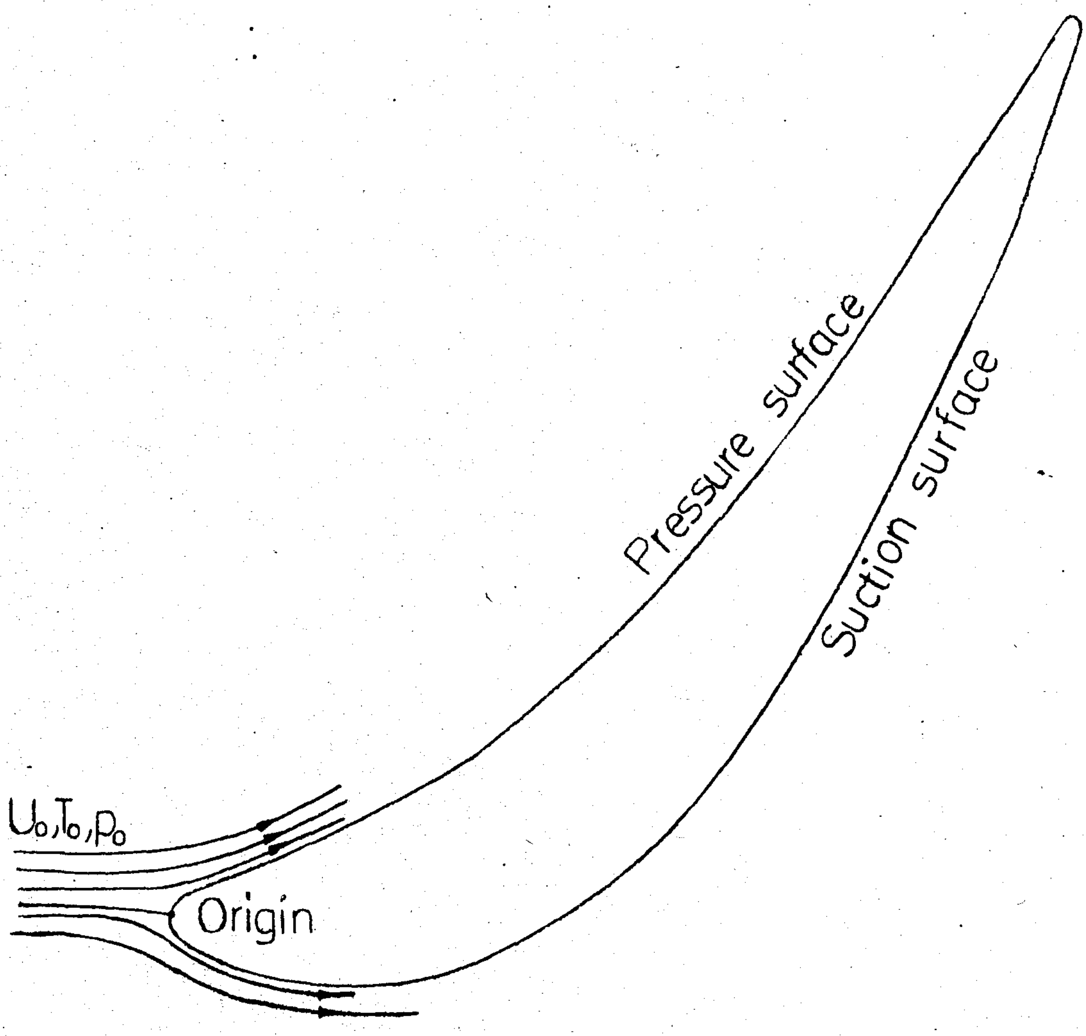

Fig.18- Inviscid flow pattern and boundary layer development around the blade

Fig. 20 and 21 show typical velocity and temperature profiles for normal injection. It is noted that, at the trailing edge of the slot, velocity and temperature profiles assume "S" shape which is an indication of adverse pressure gradient effect of injection.

TABLE 1- Film Cooling Parameter Values Used in the Study of the Film Cooling of the Blade

Cases	(kg/ms) $\dot{M}_c$	- F	(deg) α	(cm) s	(m/s) U_o	(^oK) T_c	(cm) L	(Number of Slots) n	Significance
1	1.82	0.025	84	0.183	100	750	-	1	Effects of
2	1.82	0.025	45	0.183	100	750	-	1	coolant mass
3	2.63	0.05	84	0.183	100	750	-	1	flux and injec-
4	2.63	0.05	45	0.183	100	750	-	1	tion angles
5	5.26	0.1	84	0.183	100	750	-	1	
6	5.26	0.1	45	0.183	100	750	-	1	
7	2.63	0.025	84	0.367	100	750	-	1	Slot width
8	2.63	0.05	84	0.183	100	750	-	1	effect in normal injection
9	2.63	0.025	84	0.183	200	750	-	1	Mach number
10	2.63	0.025	45	0.183	200	750	-	1	effect
11	5.26	0.05	84	0.183	200	750	-	1	
12	5.26	0.05	45	0.183	200	750	-	1	
13	2.63	0.05	84	0.183	100	500	-	1	Coolant tempera- ture effect in normal injection
14	5.26	0.1	84	0.183	100	500	-	1	
15	10.52	0.1	84	0.367	100	750	-	1	Multiple slot
16	10.52	0.1	84	0.183	100	750	3.67	2	and slot spacing
17	10.52	0.1	84	0.183	100	750	7.34	2	effects
18	15.78	0.1	84	0.183	100	750	3.67	3	
19	21.04	0.1	84	0.183	100	750	3.67	4	

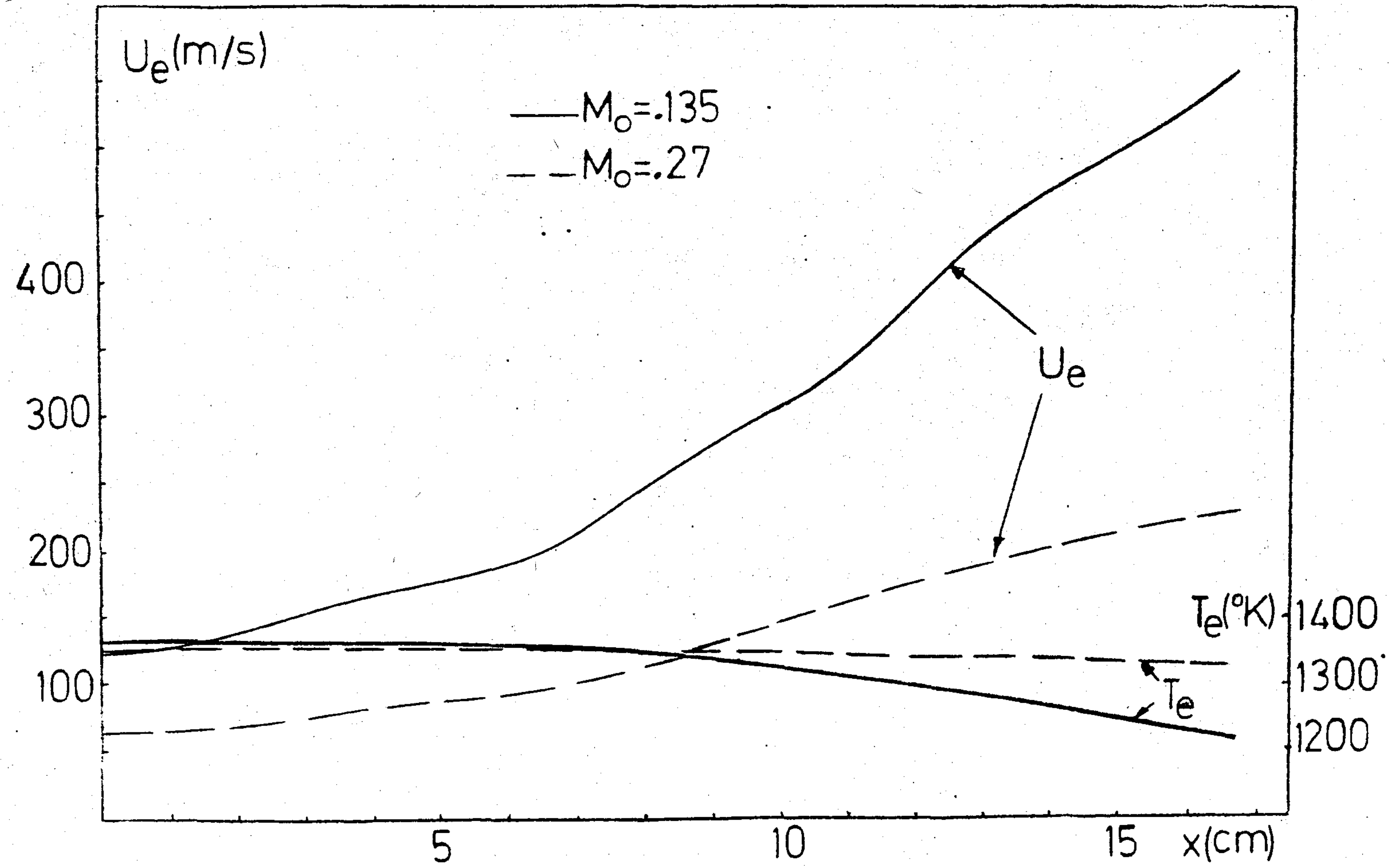

Fig.19- Outer edge velocity and temperature distributions along the pressure surface

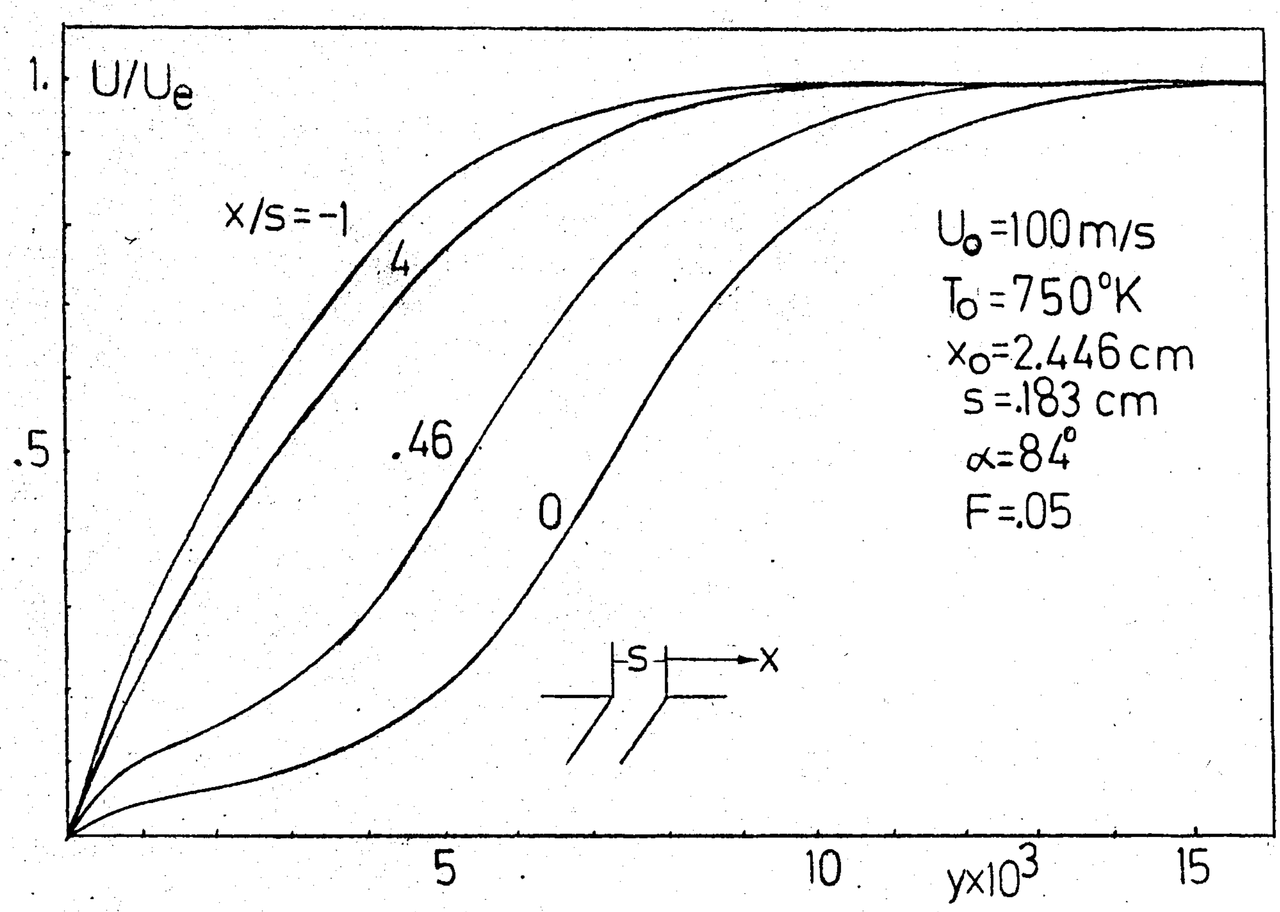

Fig.20- Velocity profiles for normal injection

Fig.22 and 23 show the influence of injection angle, α, and the coolant mass flow rate, $\dot{M}_c$, on effectiveness for M_o = 0.135 and 0.27, respectively. Normal injection and inclined injection yield the same effectiveness near the slot. Downstream of the slot, however, normal injection is more effective as in the incompressible case (Similar conclusion is reported by Nilson and Tsuei(5)). This is primarily attributed to the larger boundary layer thickness caused by

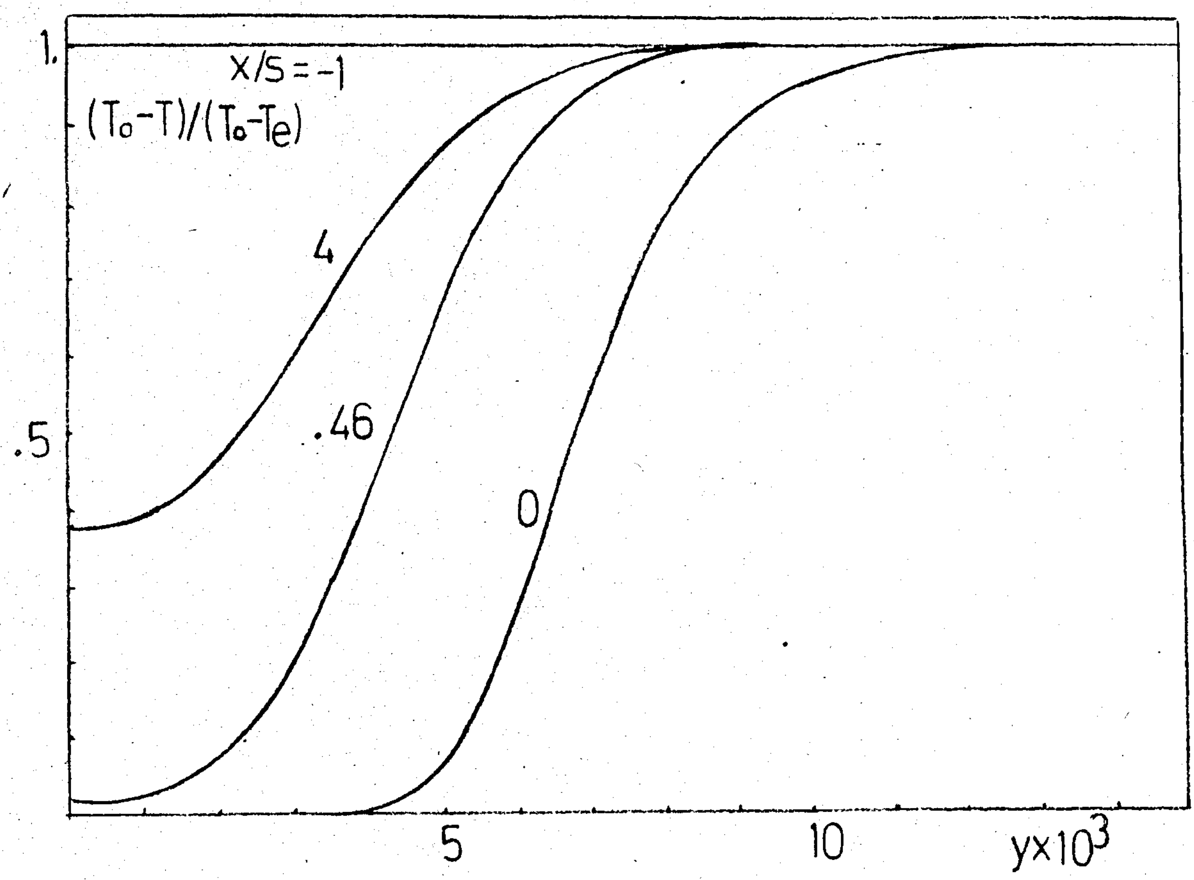

Fig.21- Temperature profiles for normal injection

normal injection. Normal injection is superior from the manufacturing and strengths points of view, as well. However, normal injection has a disadvantage. The accompanying boundary layer thickness growth increases drag and reduces aerodynamic performance. Therefore, a trade-off study may be required for the selection of injection angle.

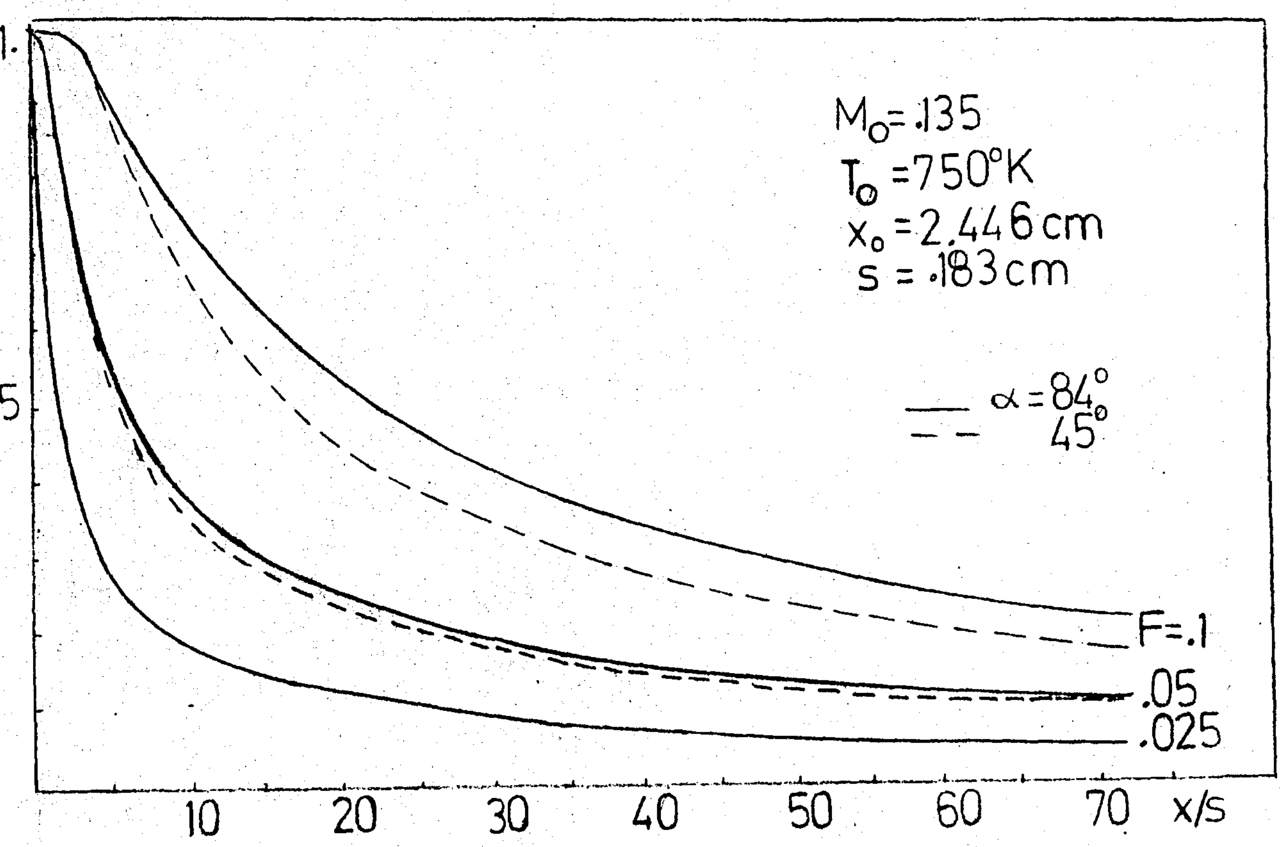

Fig.22- Comparison of effectiveness for different mass flow rates and injection angles at M_o = 0.135

Fig.24 shows the effect of varying slot width with constant mass flow rate for normal injection. As explained in the preceding section, narrow slot provides larger boundary layer thickness which is the dominant cooling mechanism for normal injection. As a result, narrow slot is more effective.

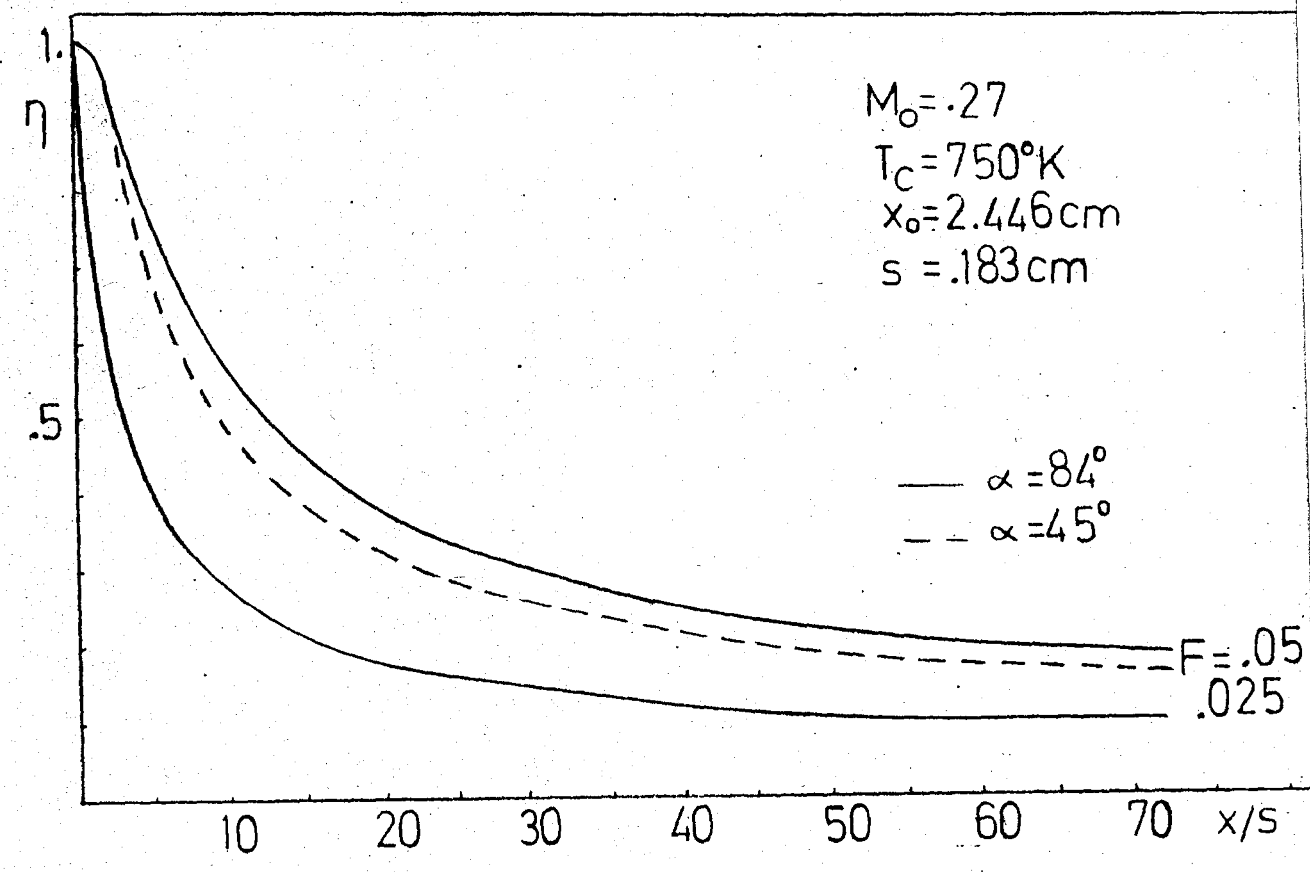

Fig.23- Comparison of effectiveness for different mass flow rates and injection angles at M_o = 0.27

Fig.25 compares film cooling effectiveness for different free stream Mach numbers (M_o = 0.135 and 0.27). In high spead flows, frictional heating causes larger boundary layer thickness (i.e., better insulation) and lower density upstream of the slot. Mainstream gas at low density near the wall can more readily be blown away from the wall by injection. Therefore, as Mach number increases, higher effectiveness is obtained. Similar result has been obtained by Nilson and Tsuei(11).

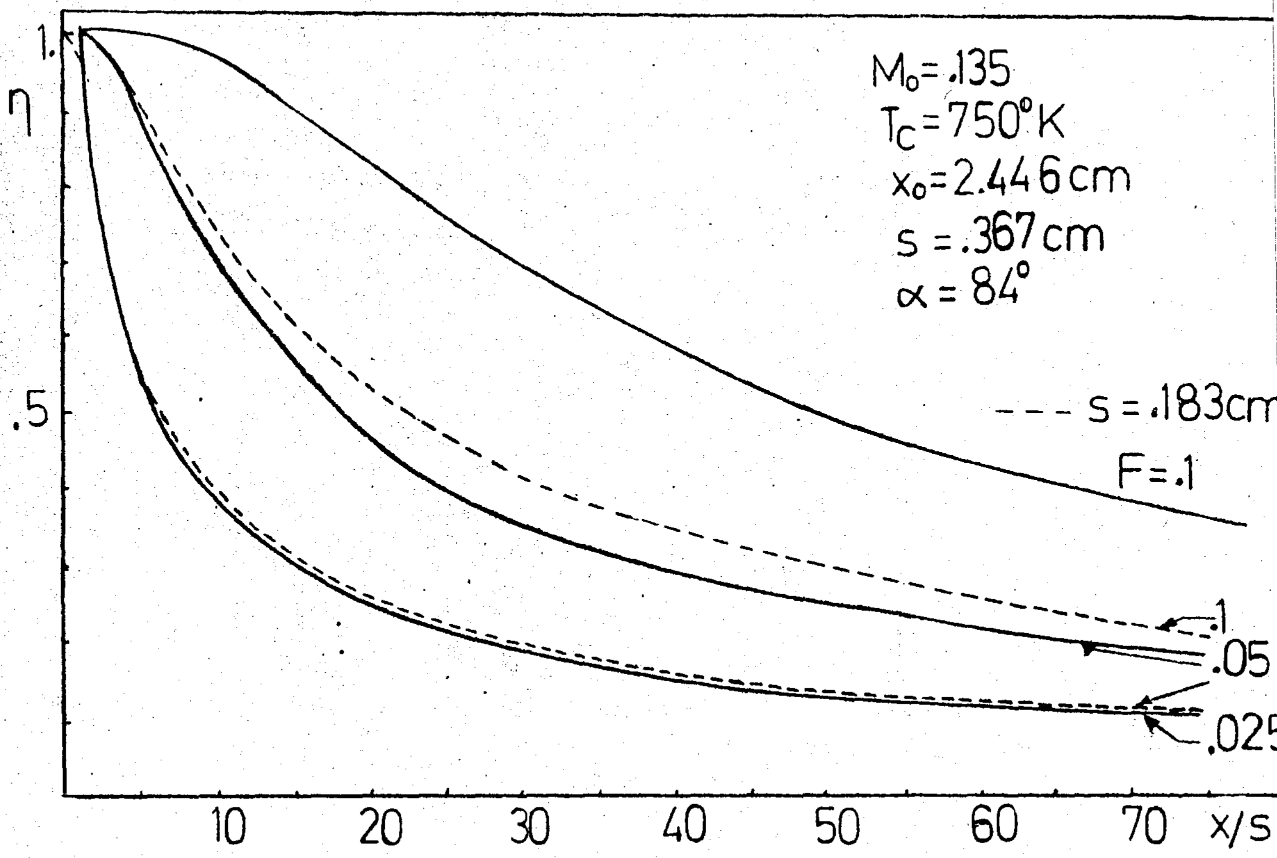

Fig.24- Slot width effect for different injection angles and injection ratios

Fig.26 illustrates the effect of coolant temperature (T_c = 500°K and 750°K) with constant coolant mass flow rate. Lower coolant temperature yields a bit lower effectiveness because lower temperature causes higher density and lower injection velocity (i.e., thinner boundary layer).

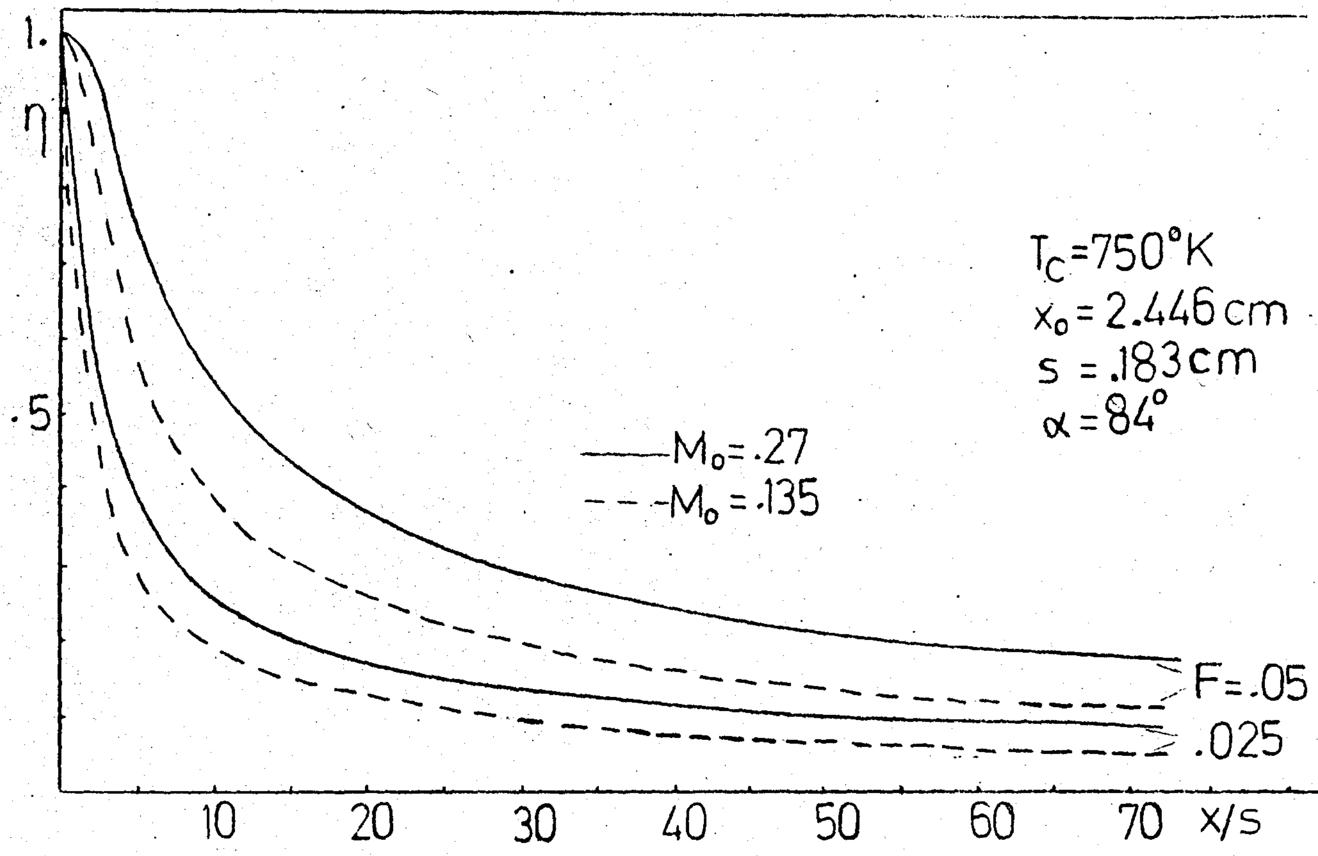

Fig.25- Comparison of effectiveness for different coolant mass flow rates and free stream Mach numbers

Fig.27 presents the effect of number of slots used and slot spacing. A single slot configuration is less effective than a double slot configuration which has the same coolant mass flow rate. However, the influence is dependent strongly on the distance, L, between the slots. To clarify this point, the second slot has been located 3.67 cm and 7.34 cm apart from the first slot, respectively. As can be noted in Fig.27, the two cases differ considerably (similar conclusion is reported by Nilson and Tsuei(11)). Use of more than two slots provides higher and more uniform effectiveness (Fig.27), at the expense of increasing boundary layer thickness and reducing aerodynamic performance.

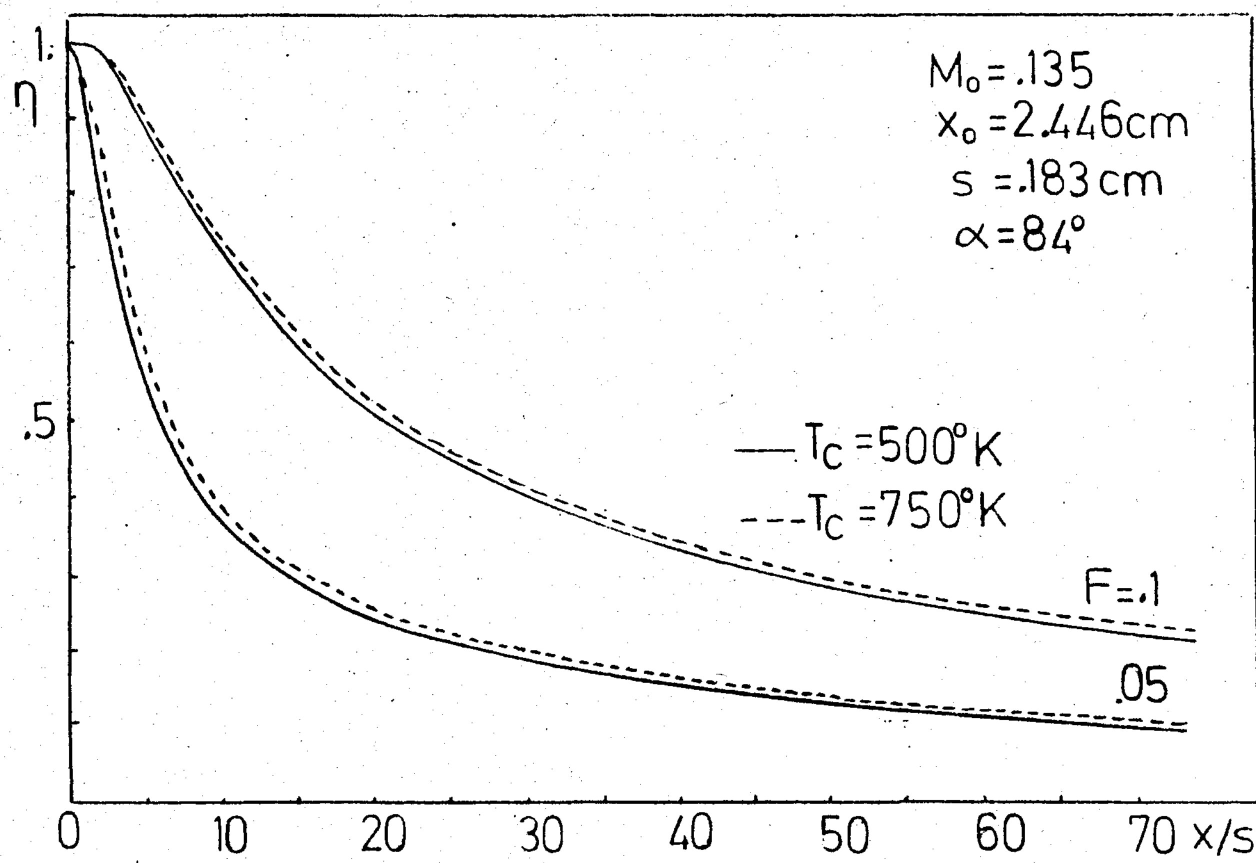

Fig.26- Comparison of effectiveness for different coolant mass flow rate and coolant temperatures

the second slot has been located 3.67 cm and 7.34 cm apart from the first slot, respectively. As can be noted in Fig.27, the two cases differ considerably (similar conclusion is reported by Nilson and Tsuei(11)). Use of more than two slots provides higher and more uniform effectiveness (Fig.27), at the expense of increasing boundary layer thickness and reducing aerodynamic performance.

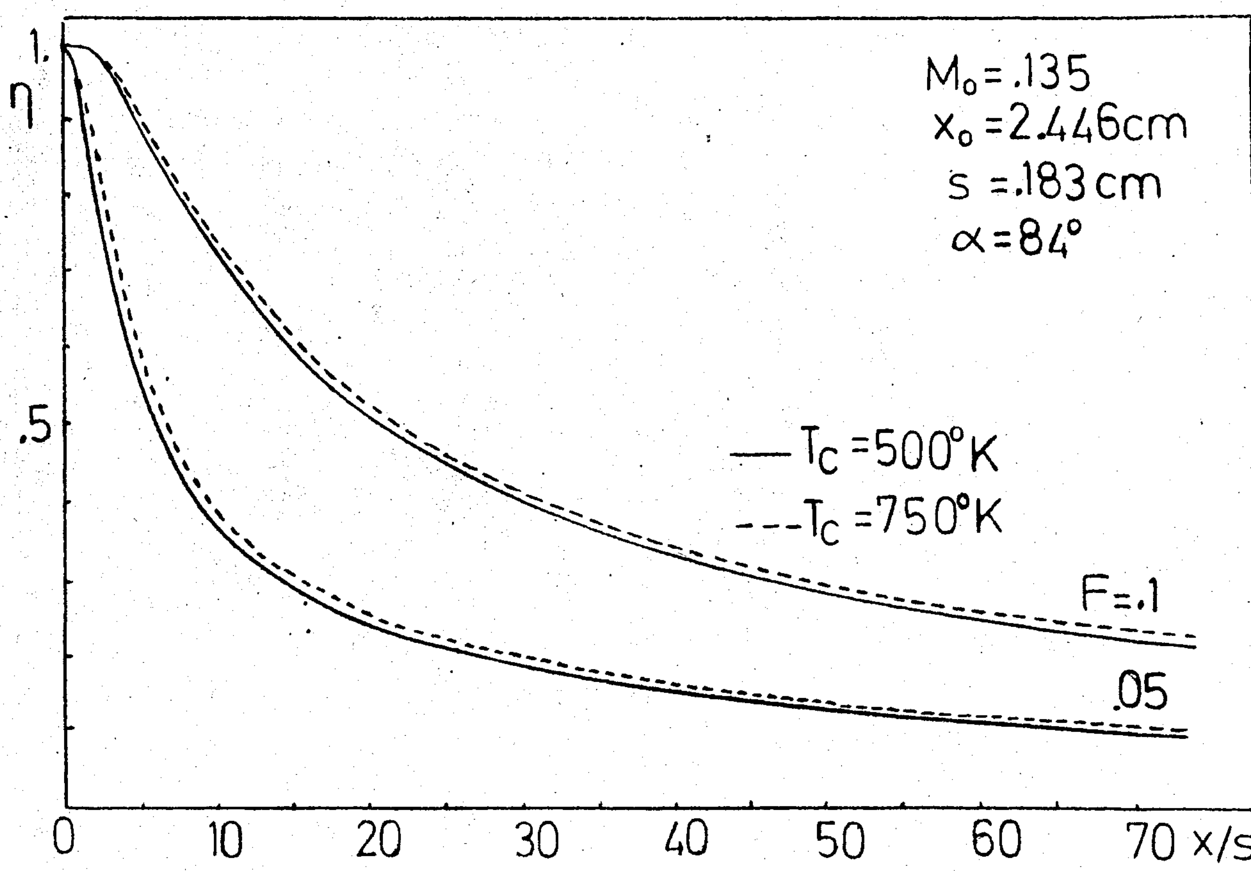

Fig.26- Comparison of effectiveness for different coolant mass flow rate and coolant temperatures

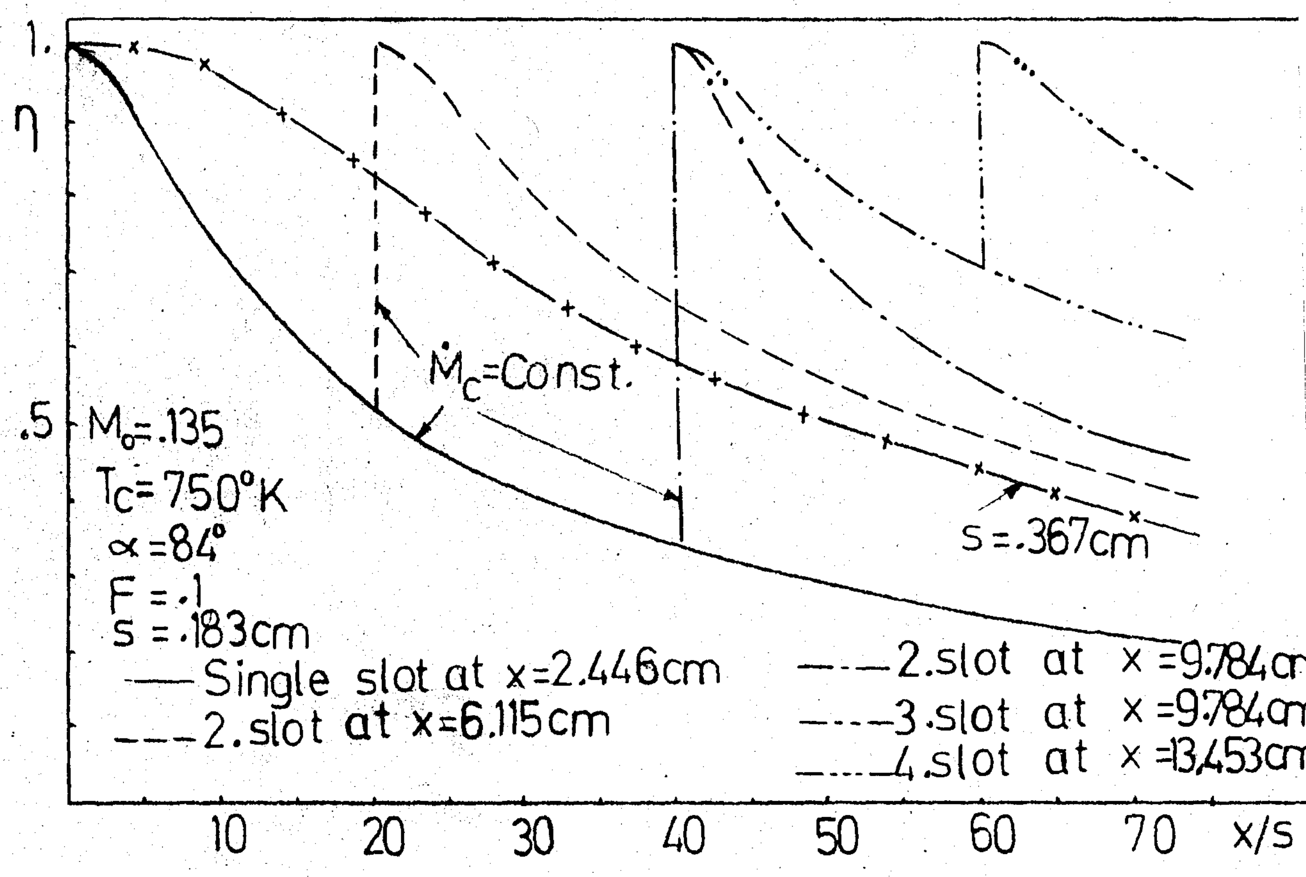

Fig.27- Comparison of effectiveness for multiple slots

CHAPTER V
CONCLUSIONS AND RECOMMENDATIONS

An investigation of laminar film couling of a single stage stator section blade of a gas turbine by oblique slot injection is presented. Numerical solutions of boundary layer equations are obtained by using a finite-difference method. The accuracy of the numerical formulation has been tested and quite satisfactory results have been obtained. The following conclusions are drawn as a result of the present study.

1- Normal injection provides greater effectiveness than inclined and tangential injection and is more suitable from the standpoints of manufacturing and blade strength. However, the accompanying boundary layer thickness growth increases drag and reduces aerodynamic performance.

2- In the case of inclined and tangential injections, wide slot yields higher effectiveness than narrow slot for the same coolant mass flow rate. However, narrow slot is more effective for normal injection.

3- Increase in free stream Mach number provides greater effectiveness. In other words, in high speed flows, higher effectiveness is achieved for the same injection rate.

4- Multiple slot cooling increases effectiveness and yields more uniform wall temperature. However, with the introduction of every slot boundary layer thickness may be increased excessively. This, in turn, reduces aerodynamic performance.

5- The present study should be continued to extend the model to turbulent flows. The primary difficulty here is the lack of an eddy viscosity model valid over a wide range of injection rates and angles as noted by Inger and Swean(12).

REFERENCES

(1) Hartnett, J.P., Birkebak, R.C. and Eckert, E.R.G., "Velocity Distributions, Temperature Distributions, Effectiveness, and Heat Transfer for Air Injected Through a Tangential Slot into a Turbulent Boundary Layer", Journal of Heat Transfer, Vol.83, 1961, pp.293-306.

(2) Haering, G.W., "Gas Film Cooling-Effects of Coolant Flow Conditions", Journal of Heat Transfer, Vol.92, 1970, p.553.

(3) Seban, R.A., "Heat Transfer for a Turbulent Boundary Layer with Tangential Fluid Injection", Journal of Heat Transfer, Vol.82, 1960, pp.303-312.

(4) Goldstein, R.J., Shavit, G. and Chen, T.S., "Film Cooling Effectiveness with Injection Through a Porous Section", Journal of Heat Transfer, Vol.87, 1965, pp.353-361.

(5) Seban, R.A. and Back, L.H., "Effectiveness and Heat Transfer for a Turbulent Boundary Layer with Tangential Injection and Variable Free-stream Velocity", Journal of Heat Transfer, Vol.84, 1962, pp.235-244.

(6) Spalding,D.B., "Prediction of Adibatic Wall Temperatures in Film Cooling Systems', AIAA Journal, Vol.3, 1965, p.965.

(7) Goldstein,R.J., "Film Cooling", Advances in Heat Transfer, Vol.7, Academic Press, N.Y., 1971, pp.321-379.

(8) Mayle,R.E. and Kopper,F.C., "Adiabatic Wall Effectiveness of a Turbulent Boundary Layer With Slot Injection", Journal of Heat Transfer, Vol.98, 1976, pp.240-244.

(9) Spalding,D.B., "Boundary-Layer Theory Applied to Film-Cooling Processes", Progres in Heat and Mass Transfer, Vol.4, Pergamon Press, New York, 1971, pp.279-296.

(10) Nilson,R.H. and Tsuei,Y.G., "Film Cooling by Oblique Slot Injection, AIAA Journal, Vol.12, 1974, pp.727-729.

(11) Nilson,R.H. and Tsuei,Y.G., "Film Cooling by Oblique Slot Injection in High Speed Laminar Flow", AIAA Journal, Vol.13, 1975, pp.1199-1202.

(12) Inger,G.R. and Swean,T.F., "Vectored Injected into Laminar Boundary Layers with Heat Transfer", AIAA Journal, Vol.13, 1975, pp.616-622.

(13) Cebeci,T. and Smith,A.M.O., "Analysis of Turbulent Boundary Layers", Academic Press, New York, 1974.

(14) Krause,E., "Numerilcal Solution of the Boundary-Layer Equations", AIAA Journal, Vol.5, 1967, pp.1231-1237.

(15) Rosenhead,L., "Laminar Boundary Layers", Oxford University Press, 1966, p.332.

(16) Wallace,J. and Kemp,N., "Similarity Solutions to the Massive Blowing Problem", AIAA Journal, Vol.7, 1969, pp.1517-1523.

(17) Hartnett,J.P. and Eckert,E.R.G., "Mass-Transfer Cooling in a Laminar Boundary Layer With Constant Fluid Properties", Recent Advances in Heat and Mass Transfer, McGraw-Hill Book Company. Inc., New York, 1961, pp.147-148.

(18) Liu,T.M. and Nachsteim,P.R., "Shooting Method for Solution of Boundary Layer Flows with Massive Blowing", AIAA Journal, Vol.11, 1973, pp.1584-1586.

(19) Liu,T.M. and Nachsteim,P.R., "Numerical Stability of Boundary Layers with Massive Blowing", AIAA Journal, Vol.11, 1973, pp.1197-1198.

(20) Inger,G.R., "Laminar Boundary-Layer Solutions with Strong Blowing", AIAA Journal, Vol.5, 1967, pp.1677-1678.

(21) Liu,T.M., "Fast and Stable Numerical Method for Boundary-Layer Flow with Massive Blowing", AIAA Journal, Vol.14, 1976, pp.114-116.

(22) Cebeci,T., Smith,A.M.O. and Wang,L.C., "A Finite Difference Method for Calculating Compressible Laminar and Turbulent Boundary Layers', Mc Donnel Douglas Aircraft Company, Inc., Report No.OAC-67131, Parts 1 and 2, 1969.

(23) Katsanis,T., "Fortran Program for Calculation Transonic Velocities on a Blade-to-Blade Stream Surface of a Turbomachine", NASA T.No D-5427, 1969.

(24) Schlichting,H., "Boundary Layer Theory", Mc Graw-Hill Book Company, Inc., New York, 1968.

APPENDICES

A. APPROXIMATION OF DERIVATIVES BY FINITE DIFFERENCE METHOD

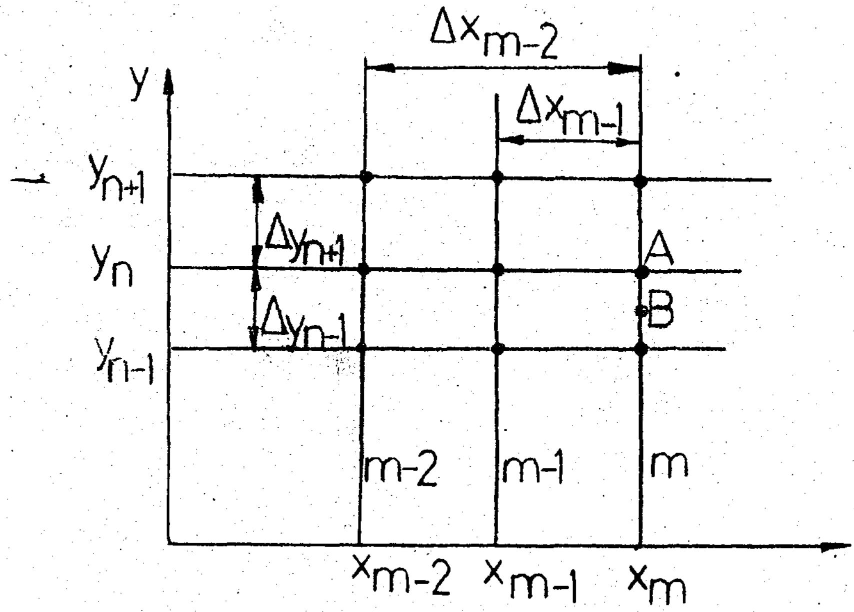

Fig.28- System of nodal points used in the finite difference formulation

Using the mesh shown in Fig.28, partial derivatives at point A can be approximated as follows (All quantities are in their dimensionless form):

Three point difference:

$$\left.\frac{\partial U}{\partial x}\right|_{m,n} = H_m U_{m-2,n} - I_m U_{m-1,n} + J_m U_{m,n} + O(\Delta x^2)$$

Backward difference:

$$\left.\frac{\partial U}{\partial x}\right|_{m,n} = \frac{U_{m,n} - U_{m-1,n}}{\Delta x_{m-1}} - O(\Delta x)$$

Central difference:

$$\frac{\partial U}{\partial y}\bigg|_{m,n} = K_n U_{m,n+1} - L_n U_{m,n-1} + M_n U_{m,n}$$

$$\frac{\partial^2 U}{\partial y^2}\bigg|_{m,n} = P_n U_{m,n+1} + R_n U_{m,n-1} - S_n U_{m,n} - 0(\Delta y^2)$$

<u>Approximation at the point B</u>

Central difference:

$$\frac{\partial V}{\partial y}\bigg|_{m,n-\frac{1}{2}} = \frac{V_{m,n} - V_{m,n-1}}{\Delta y_{n-1}} - 0\ (\Delta y^2)$$

Central + three point difference:

$$\frac{\partial U}{\partial x}\bigg|_{m,n-\frac{1}{2}} = \frac{1}{2}\Big[H_m(U_{m-2,n} + U_{m-2,n-1}) + I_m(U_{m-1,n} + U_{m-1,n-1}) + J_m(U_{m,n-1} + U_{m,n})\Big]$$

Central + backward difference:

$$\frac{\partial U}{\partial x}_{m,n} = \frac{1}{2}\ \frac{U_{m,n} + U_{m,n-1} - U_{m-1,n} - U_{m-1,n-1}}{\Delta x_{m-1}}$$

where, subscript m stands for station number and n for the nodal point at the station considered and where

$$\Delta x_{m-1} = x_m - x_{m-1} \qquad \Delta x_{m-2} = x_m - x_{m-2}$$

$$\Delta y_{n+1} = y_{n+1} - y_n \qquad \Delta y_{n-1} = y_n - y_{n-1}$$

$$H_m = \frac{\Delta x_{m-1}}{(x_{m-1} - x_{m-2})\Delta x_{m-2}} \qquad I_m = \frac{\Delta x_{m-2}}{(x_{m-1} - x_{m-2})\Delta x_{m-1}}$$

$$J_m = \frac{1}{\Delta x_{m-2}} + \frac{1}{\Delta x_{m-1}} \qquad K_n = \frac{\Delta y_{n-1}}{\Delta y_{n+1}(y_{n+1}-y_{n-1})}$$

$$L_n = \frac{y_{n+1}}{\Delta y_{n-1}(y_{n+1}-y_{n-1})} \qquad M_n = \frac{1}{\Delta y_{n-1}} - \frac{1}{\Delta y_{n+1}}$$

$$P_n = \frac{2}{\Delta y_{n+1}(y_{n+1}-y_{n-1})} \qquad R_n = \frac{2}{\Delta y_{n-1}(y_{n+1}-y_{n-1})}$$

$$S_n = \frac{2}{\Delta y_{n-1}\Delta y_{n+1}}$$

$\frac{\partial T}{\partial x}$, $\frac{dP}{dx}$, $\frac{\partial T}{\partial y}$, $\frac{\partial \mu}{\partial y}$, $\frac{\partial}{\partial y}(\frac{\mu}{Pr})$ and $\frac{\partial^2 T}{\partial y^2}$ are approximated in similar manner.

B. DIFFERENCE EQUATIONS

I- Momentum Equation and Solution Procedure

Upon substituting corresponding expansions of partial derivatives into the momentum equation, the following recursion formula is obtained:

$$B_n U_{n+1} + C_n U_n + D_n U_{n-1} = E_n \qquad 2 \leq n \leq N-1$$

where U_n denotes tangential velocity at nodal points across the station x_m. B_n, C_n, D_n and E_n all consist of known values (assumed profiles + upstream data) and are given as:

$$B_n = K_n(V_n^a - B_n') - P_n \frac{\mu_n^a}{\rho_n^a \; Re}$$

$$C_n = J_m U_n^a + M_n (V_n^a - B_n') + S_n \frac{\mu_n^a}{\rho_n^a \ Re}$$

$$D_n = -L_n (V_n^a - B_n') - R_n \frac{\mu_n^a}{\rho_n^a \ Re}$$

$$E_n = U_n^a (I_m U_{m-1,n} - H_m U_{m-2,n}) - \frac{1}{\rho_n^a} (H_m p_{m-2} - I_m p_{m-1} + J_m p_m)$$

where

$$B_n' = \frac{1}{\rho_n^a \ Re} (K_n \ \mu_{n+1}^a - L_n \mu_{n-1}^a + \mu_n^a \ M_n)$$

and superscript 'a' denotes assumed values.

When use is made of simple backward difference, the first term in C_n is replaced by

$$\frac{U_n^a}{\Delta x_{m-1}}$$

E_n is replaced by

$$E_n = \frac{U_{m-1,n}}{\Delta x_{m-1}} U_n^a - \frac{1}{\rho_n^a} \left(\frac{p_m - p_{m-1}}{\Delta x_{m-1}}\right)$$

With the aid of boundary conditions

$$\text{At} \quad y=0 \quad U=U_w \begin{cases} 0 \\ U_c \end{cases}$$

$$\text{At} \quad y \to \infty \quad U=U_e$$

the above recursion formula is readily converted into three-block diagonal matrix equation.

$$
\begin{bmatrix}
C_2 & B_2 & & & 0 \\
D_3 & C_3 & B_3 & & \\
 & & \ddots & & \\
 & & D_{N-2} & C_{N-2} & B_{N-2} \\
0 & & & D_{N-1} & C_{N-1}
\end{bmatrix}
\begin{bmatrix}
U_2 \\ U_3 \\ \vdots \\ U_{N-2} \\ U_{N-1}
\end{bmatrix}
=
\begin{bmatrix}
E_2 - D_2 U_w \\ E_3 \\ \vdots \\ E_{N-2} \\ E_{N-1} - B_{N-1} U_e
\end{bmatrix}
=
\begin{bmatrix}
E'_2 \\ E'_3 \\ \vdots \\ E'_{N-2} \\ E'_{N-1}
\end{bmatrix}
$$

This matrix equation can be solved by Gaussian elimination method. Since the coefficient matrix is of three-block diagonal type, unknowns can readily be determined by the following procedure.

First, coefficients are modified as:

$$C_{n+1} \rightarrow C_{n+1} - \frac{B_n D_{n+1}}{C_n} \qquad n = 2, N-2$$

$$E'_{n+1} \rightarrow E'_{n+1} - \frac{E'_n D_{n+1}}{C_n} \qquad n = 2, N-2$$

For example,

$$C_3 \rightarrow C_3 - \frac{B_2 D_3}{C_2} \qquad E'_3 \rightarrow E'_3 - \frac{E'_2 D_3}{C_2}$$

$$C_4 \rightarrow C_4 - \frac{B_3 D_4}{C_3} \qquad E'_4 \rightarrow E'_4 - \frac{E'_3 D_4}{C_3}$$

(Note that modified form of C_3 and E'_3 are utilized to evaluate new C_4 and E'_4).

Then, U_n's can be calculated by the following recursion formula:

$$U_{N-1} = E'_{N-1}/C_{N-1}$$

$$U_n = (E'_n - B_n U_{n+1})/C_n \qquad n = N-2, 2$$

II- <u>Continuity Equation</u>

Difference form of continuity equation centered at point B (Fig.28) is:

$$V_n = \frac{1}{\rho_n^a}\left(V_{n-1}\rho_{n-1}^a - \frac{\Delta y_{n-1}}{2}\left[H_m\left(U_{m-2,n}\rho_{m-2,n} + U_{m-2,n-1}\rho_{m-2,n-1}\right)\right.\right.$$
$$\left.\left. - I_m(U_{m-1,n}\rho_{m-1,n} + U_{m-1,n-1}\rho_{m-1,n-1}) + J_m(U_n\rho_n^a + U_{n-1}\rho_{n-1}^a)\right]\right)$$

or (backward difference)

$$V_n = \frac{1}{\rho_n^a}\left(V_{n-1}\rho_{n-1}^a - \frac{\Delta y_{n-1}}{2\Delta x_{m-1}}(U_n\rho_n^a + U_{n-1}\rho_{n-1}^a - U_{m-1,n}\rho_{m-1,n}\right.$$
$$\left. - U_{m-1,n-1}\rho_{m-1,n-1})\right)$$

$$2 \leq n \leq N-1$$

Appropriate boundary conditions:

$$V_1 = V_w \begin{cases} 0 \\ V_c \end{cases}$$

III- Energy Equation

When approximated forms of derivatives are substituted into the energy equation, a three-block diagonal matrix results similar to that for the momentum equation:

$$T_{n+1}\bar{B}_n + T_n\bar{C}_n + T_{n-1}\bar{D}_n = \bar{E}_n \qquad 2 \leq n \leq N-1$$

where T_n's denote dimensionless temperature at nodal points across the station, x_m.

$\bar{B}_n$, $\bar{C}_n$, $\bar{D}_n$ and $\bar{E}_n$ all consist of computed values from momentum and continuity equation and, of assumed values. Coefficients of energy equation differ slightly from those of momentum equation. Therefore, by the following substitutions, $\bar{B}_n$, $\bar{C}_n$ and $\bar{D}_n$ can easily be obtained from B_n, C_n and D_n.

$$V_n^a \rightarrow V_n$$

$$U_n^a \rightarrow U_n$$

$$\mu_n^a \rightarrow \mu_n^a / Pr_n^a$$

where Pr_n^a stands for Prandtl number at nodal points. $\bar{E}_n$'s, however, differ due to viscous dissipation term and pressure gradient term. Therefore, it is given separately as:

$$\bar{E}_n = U_n(I_m T_{m-1,n} - H_m T_{m-2,n}) + E \frac{U_n}{\rho_n^a}(H_m p_{m-2} - I_m p_{m-1} + J_m p_m) + \phi_n$$

where ϕ_n accounts for viscous dissipation term

$$\phi_n = E(K_n U_{n+1} - L_n U_{n-1} + M_n U_n)^2 \frac{\mu_n^a}{\rho_n^a \, Re_o}$$

or (backward difference)

$$\bar{E}_n = U_n \frac{T_{m-1,n}}{\Delta x_{m-1}} + E \frac{U_n}{\rho_n^a} \frac{(p_m - p_{m-1})}{\Delta x_{m-1}} + \phi_n .$$

Note that E with no subscript stands for Eckert number.

Difference equation for energy equation is solved by the above method using the following boundary conditions.

$$\text{At} \quad y=0 \quad \begin{cases} T=T_w \quad \text{(dimensionless)} \\ \dfrac{\partial T}{\partial y} = 0 \end{cases}$$

$$\text{At} \quad y\to\infty \quad \{T=T_e$$

Adiabatic wall condition can be expanded by three-point difference scheme, thus following relationship is obtained among T_1, T_2 and T_3.

$$T_1 = \frac{(\Delta y_1 + \Delta y_2)^2 T_2 - \Delta_{y1}^2 T_3}{\Delta y_2 \, (2\Delta y_1 + \Delta y_2)}$$

For adiabatic wall condition, coefficient matrix changes slightly as:

$$\bar{C}_2 \to \bar{C}_2 + \bar{D}_2 \frac{(1 + k)^2}{2(2 + k)} , \quad \bar{B}_2 \to \bar{B}_2 - \frac{\bar{D}_2}{k(2+k)}$$

where k is magnification factor.

For incompressible flow over flat plate, simply take

$$\rho_n^a = \rho_{m-1,n} = \rho_{m-2,n} = \mu_n^a = 1, \quad Pr_n^a = Pr = \text{constant}.$$

$$U_e = T_e = p_m = p_{m-1} = 1$$

and carry out necessary reductions (e.g., pressure terms and B'_n vanish) in all difference equations.

C. CONVERGENCE CRITERION

Since the boundary layer equations are non-linear iteration is necessary. If the relative error based on the computed and the assumed values is less than the desired value, say ϵ, then iteration is stopped. In other words, iterations are continued until the following condition is satisfied:

$$\left| 1 - \frac{\bar{U}_n^c}{\bar{U}_n^a} \right| < \epsilon$$

Iteration can also be carried out over $\bar{T}$ or $\bar{v}$ but they may have undesirable values (e.g., zero or almost zero) during the calculations. Therefore, iteration is repeated over $\bar{U}$ but relative error based on temperature is also observed.

In all calculations, $\epsilon = 0.0005$ was used.

D. COMPUTER PROGRAM

The list of the computer program used to solve boundary layer equations are presented on the following pages:

```
      DIMENSION EETA(90),DDF(90),FF(90),U(2,90),V(2,90),XU(90),
     $XV(90),C(90),B(90),E(90),D(90),A(90,90),UU(90),VV(90)
     $,UUU(90),XX(3),YY(90),P(90),AA(90),BB(90),CC(90),DD(90),
     $EE(90),DYM1(90),DYP1(90),TT(90),T(2,90),TTT(90),VISDIS
     $(90),DYPM(90),FG(90),IN(200),TINF(200),UINF(200),PRES(200)
     $,RHO1(90),RHO2(90),TRED1(90),XNU(90),TRED(90),XMU(90),RHO
     $(90),XT(90),TRED2(90),X1(200),UE1(200),XSURF(200),TTEMP(200)
     $,PRSS(200),YCORD1(90),YCORD2(90),VEL1(90),VEL2(90),TEMP1(90)
     $,TEMP2(90),XW(90),PRNO(90),XXL(15),TTE(90),UUE(90),VVE(90)
      REAL    MRATIO,MTP
      DOUBLE  PRECISION  A,UUU,E,TTT
      READ(5,521)ICOMP,IFLAT,ICONT,JPRINT,IFILE,IR,IW,MSTART,MJ,
     $NSTART,NDIV,NSTEP,NSTEP1,NSTOP,M,NMAX,NNMAX
  521 FORMAT(4I1,13I3)
      READ(5,83)XST,ALFA,CHORD,DXSL,SL,YMAX,DX
      READ(5,83)MRATIO,U0,RE,TT0,TCOOL
      READ(5,491)(EETA(I),DDF(I),I=1,22)
   83 FORMAT(8F10.0)
  491 FORMAT(3(2F10.0))
      K=7
      IFIRST=1
      ISECND=2
      EPS=.0005
      ALFA1=ALFA
      ALFA=ALFA*4.*ATAN(1.)/180.
      TRATIO=TCOOL/TT0
      MTP=MRATIO*TRATIO*COTAN(ALFA)
      IF(ICOMP.EQ.0)MTP=MRATIO*COTAN(ALFA)
      DXP=DX
      TMEAN=(TCOOL+TT0)/2.
      PRO=AITINT(EETA,DDF,22,TMEAN,K,P)
      PRESO=(1717.9*1.8*TT0)/U0**2
      ECK=U0**2/(6035.*(TT0-TCOOL)*1.8)
      WRITE(6,524)
      WRITE(6,525)M,NDIV,NSTART,MJ,NNMAX,NMAX,NSTEP,NSTOP,ICONT,
     $IFILE,MSTART,SL,EPS,YMAX,RE,ECK,U0,CHORD,PRESO,
     $TCOOL,TT0,XST,DXSL,MRATIO,ALFA1
  524 FORMAT(///,20X,' I N P U T     D A T A  ',/)
  525 FORMAT(/////,10X,'M=',I3,2X,'NDIV=',I3,2X,'NSTART=',I3,
     $5X,'MJ=',I3,3X,'NNMAX=',I3,3X,//,7X,'NMAX=',I3,1X,'NSTEP=',
     $I3,2X,'NSTOP=',I3,1X,'ICONT=',I2,2X,'IFILE=',I3,2X,
     $'MSTART=',I3,2X,////,10X,
     $'SL=',F4.2,9X,'EPS=',F8.6,5X,'YMAX=',F10.7,3X,'RE=',F10.3,
     $5X,//,9X,'ECK=',F10.8,4X,'U0=',F7.3,5X,'CHORD=',F8.6,2X,
     $'PRESO=',F10.5,5X,//,7X,'TCOOL=',F6.2,7X,'TT0=',F10.4,4X,
     $'XST=',F7.5,4X,'DXSL=',F7.5,5X,//,6X
     $,'MRATIO=',F6.4,6X,'ALFA=',F6.2,5X,/////)
      MMAX=M
      TRDUC=1.+110./TT0
      TRDCE=110./TT0
      YY(1)=0.
      DY=YMAX*(SL-1.)/(SL**(M-1)-1.)
      JINT=2
      DO 76 J=JINT,M
   76 YY(J)=DY*(SL**(J-1)-1.)/(SL-1.)
      DO 77 J=JINT,M-1
      DYM1(J)=YY(J)-YY(J-1)
      DYP1(J)=YY(J+1)-YY(J)
      DYPM(J)=DYM1(J)+DYP1(J)
      AA(J)=DYM1(J)/DYP1(J)/DYPM(J)
      BB(J)=2./DYP1(J)/DYPM(J)
      CC(J)=1./DYM1(J)-1./DYP1(J)
      DD(J)=2./DYM1(J)/DYP1(J)
      EE(J)=DYP1(J)/DYPM(J)/DYM1(J)
      FG(J)=2./DYM1(J)/DYPM(J)
   77 CONTINUE
      WRITE(6,110)
      WRITE(6,71)(I,YY(I),I=1,MMAX)
      IF(IFLAT.EQ.1)GO TO 660
      DO 301 I=1,NMAX
      READ(8,400)X1(I)
      READ(10,400)UE1(I)
      XSURF(I)=X1(I)/CHORD
      UE1(I)=UE1(I)/U0
      TTEMP(I)=1.+ECK*(1.-UE1(I)**2)/2.
  301 PRSS(I)=((1.-TTEMP(I))*TRATIO+TTEMP(I))**3.5
      PRINT*,'
      PRINT*,'                 DIM.LESS  OUTER  EDGE TEMP.  '
      WRITE(6,71)(I,TTEMP(I),I=1,NMAX)
      PRINT*,'
      PRINT*,'                 NORMALIZED PRES. GRADIENT'
      WRITE(6,71)(I,PRSS(I),I=1,NMAX)
```

```
      PRINT*,'
      PRINT*,'               SURFACE COORD.S (FT.)
      WRITE(6,71)(I,X1(I),I=1,NMAX)
      PRINT*,'
      PRINT*,'               DIM.LESS  OUTER EDGE VEL.'
      WRITE(6,71)(I,UE1(I),I=1,NMAX)
 660  CONTINUE
      XX(1)=XST
      XX1=XX(1)
      XX(2)=XX(1)+DX
      XX2=XX(2)
      XX(3)=XX(2)+DX
      XX3=XX(3)
      IF(IFLAT.EQ.1)GO TO 661
      UINF(1)=AITINT(XSURF,UE1,NMAX,XX1,K,P)
      UINF(2)=AITINT(XSURF,UE1,NMAX,XX2,K,P)
      UINF(3)=AITINT(XSURF,UE1,NMAX,XX3,K,P)
      DO  653  I=1,3
      TINF(I)=1.+ECK*(1.-UINF(I)**2)/2.
 653  PRES(I)=((1.-TINF(I))*TRATIO+TINF(I))**3.5
      GO TO 667
 661  DO 662 I=1,3
      UINF(I)=1.
      TINF(I)=1.
 662  PRES(I)=1.
 667  CONTINUE
      IF(ICONT.NE.0)GO TO 511
      DO 404 I=1,NNMAX
      READ(12,402)YCORD1(I),VEL1(I)
      READ(13,402)YCORD2(I),VEL2(I)
      READ(14,400)TEMP1(I)
      READ(15,400)TEMP2(I)
      YCORD1(I)=YCORD1(I)/CHORD
      YCORD2(I)=YCORD2(I)/CHORD
      VEL1(I)=VEL1(I)*UINF(1)
      VEL2(I)=VEL2(I)*UINF(2)
      TEMP1(I)=TEMP1(I)/6035.
      TEMP2(I)=TEMP2(I)/6035.
      TEMP1(I)=(TEMP1(I)*5./9.-TCOOL)/(TTO-TCOOL)
 404  TEMP2(I)=(TEMP2(I)*5./9.-TCOOL)/(TTO-TCOOL)
      GO TO  2023
      PRINT*,'YCORD1  AND   VEL1'
      WRITE(6,71)(I,YCORD1(I),I=1,NNMAX)
      WRITE(6,71)(I,VEL1(I),I=1,NNMAX)
      PRINT*,'YCORD2 AND  VEL2'
      WRITE(6,71)(I,YCORD2(I),I=1,NNMAX)
      WRITE(6,71)(I,VEL2(I),I=1,NNMAX)
      PRINT*,'TEMP1  AND  TEMP2'
      WRITE(6,71)(I,TEMP1(I),I=1,NNMAX)
      WRITE(6,71)(I,TEMP2(I),I=1,NNMAX)
2023  CONTINUE
 400  FORMAT(1X,D14.9)
 402  FORMAT(1X,2D14.9)
 511  CONTINUE
      ISTN=ISECND+1
      IF(ICONT.NE.0)GO TO 512
      M=MSTART
      DO 405 I=1,M
      YINT=YY(I)
      IF(YINT.GT.YCORD1(NNMAX))GO TO 407
      T(1,I)=AITINT(YCORD1,TEMP1,NNMAX,YINT,K,P)
      U(1,I)=AITINT(YCORD1,VEL1,NNMAX,YINT,K,P)
       GO TO 411
 407  U(1,I)=UINF(1)
      T(1,I)=TINF(1)
 411  CONTINUE
      IF(YINT.GT.YCORD2(NNMAX))GO TO 408
      U(2,I)=AITINT(YCORD2,VEL2,NNMAX,YINT,K,P)
      T(2,I)=AITINT(YCORD2,TEMP2,NNMAX,YINT,K,P)
      GO TO 405
 408  U(2,I)=UINF(2)
      T(2,I)=TINF(2)
 405  CONTINUE
      GO TO 513
 512  CONTINUE
      READ(IR,514)M,(U(1,I),U(2,I),T(1,I),T(2,I),V(2,I),I=1,M)
 514  FORMAT(1X,I3/(5F10.6))
 513  IN(1)=M
      IN(2)=M
      DO 22 N=1,2
      WRITE(6,84)N
  84  FORMAT(10X,/,'INITIAL VELOCITY PROFILE (U/UO)  STATION NO.=',I3
      WRITE(6,71)(J,U(N,J),J=1,M)
```

```
      PRINT*,'                INITIAL TEMPERATURE PROFILE (T-TC)/(TO-TC)
      WRITE(6,71)(J,T(N,J),J=1,M)
   22 CONTINUE
      MNO=3
      DXM1=XX(3)-XX(2)
      IF(ICOMP.EQ.0)GO TO 900
       DO 300 I=1,M
       TRED1(I)=T(1,I)+(1.-T(1,I))*TRATIO
       TRED2(I)=T(2,I)+(1.-T(2,I))*TRATIO
       RHO1(I)=PRES(1)/TRED1(I)
  300  RHO2(I)=PRES(2)/TRED2(I)
      GO TO 901
  900 DO 902 I=1,M
      RHO1(I)=1.
  902 RHO2(I)=1.
  901 CONTINUE
      U(1,1)=0.
      U(2,1)=0.
      V(2,1)=0.
      IF(ICONT.EQ.0)GO TO 2024
      PRINT*,'
      PRINT*,'                NORMAL COMP. OF VEL. AT 2.ST. (V/UO)   '
 2024 CONTINUE
      IF(ICONT.NE.0)GO TO 515
      DO 406 I=2,M
  406 V(2,I)=0.
  515 CONTINUE
      IF(ICONT.EQ.0)GO TO 2025
      WRITE(6,71)(I,V(2,I),I=1,M)
 2025 CONTINUE
   51 DELX=XX(2)-XX(1)
      MNM=MNO-1
      DXM2=XX(3)-XX(1)
      DXM1=XX(3)-XX(2)
      XLC=DXM2/DELX/DXM1
      XLD=DXM1/DELX/DXM2
      XLE=1./DXM1+1./DXM2
      M1=IN(MNM)
      M2=IN(MNM-1)
      NITE=0
      DPRES=PRESO*(XLD*PRES(MNO-2)-XLC*PRES(MNO-1)+XLE*PRES(MNO))
      DPRESA=(PRES(MNO)-PRES(MNO-1))/DXM1*PRESO
      UC1=MTR/PRES(MNO-2)
      UC2=MTR/PRES(MNO-1)
      UUC=MTR/PRES(MNO)
      U(1,1)=0.
      IF((MNO-1).GE.NSTART.AND.(MNO-2).LT.NDIV)U(1,1)=UC1
      U(2,1)=0.
      IF(MNO.GE.NSTART.AND.(MNO-1).LT.NDIV)U(2,1)=UC2
      IF(MNO.GE.NSTART.AND.(MNO-1).LT.NDIV)T(2,1)=0.
      UU(1)=0.
      IF(MNO.GE.NSTART.AND.MNO.LE.NDIV)UU(1)=UUC
      UW=UU(1)
      VV(1)=0.
      IF(ICOMP.EQ.0)TRATIO=1.
      IF(MNO.GE.NSTART.AND.MNO.LE.NDIV)VV(1)=MRATIO*TRATIO/PRES(MN
      IF(MNO.GT.MJ)GO TO 649
      IF(ABS(1.-U(2,M1-1)/UINF(MNM)).GT..000015)M=M+1
  649 IN(MNO)=M
      DO 50 I=2,M1-1
      XT(I)=T(2,I)
      XU(I)=U(2,I)
   50 XV(I)=V(2,I)
      IF(M.GT.M1)GO TO 651
      GO TO 652
  651 DO 304 I=M1,M
      U(2,I)=UINF(MNM)
      V(2,I)=V(2,I-1)
      RHO2(I)=PRES(MNM)/(TINF(MNM)+(1.-TINF(MNM))*TRATIO)
      XU(I)=U(2,I)
      XV(I)=V(2,I)
      T(2,I)=TINF(MNM)
      XT(I)=T(2,I)
      U(1,I)=UINF(MNM-1)
      RHO1(I)=PRES(MNM-1)/(TINF(MNM-1)+(1.-TINF(MNM-1))*TRATIO)
  304 T(1,I)=TINF(MNM-1)
  652 CONTINUE
      XT(1)=T(2,1)
      XT(M)=TINF(MNO)
   52 CONTINUE
      IF(ICOMP.EQ.0)GO TO 905
      DO 302 I=1,M
```

```
      TRED(I)=XT(I)+(1.-XT(I))*TRATIO
      TTINT=(XT(I)*(TTO-TCOOL)+TCOOL)*1.8
      PRNO(I)=AITINT(EETA,DDF,22,TTINT,K,P)
      XTRD=TRED(I)
      RHO(I)=PRES(MNO)/XTRD
  302 XMU(I)=XTRD*SQRT(XTRD)*TRDUC/(XTRD+TRDCE)
      DO 310 I=2,M-1
  310 XV(I)=XV(I)-1./RHO(I)/RE*(XMU(I+1)*AA(I)-XMU(I-1)*FE(I)
     $+XMU(I)*CC(I))
      GO TO 906
  905 CONTINUE
      IF(NITE.GT.1)GO TO 906
      DO 907 I=1,M
      PRNO(I)=PRO
      XMU(I)=1.
  907 RHO(I)=1.
  906 CONTINUE
      DO 53 I=2,M-1
      XNU(I)=XMU(I)/RHO(I)/RE
      B(I)=XV(I)*AA(I)-BB(I)*XNU(I)
      D(I)=-XV(I)*FE(I)-FG(I)*XNU(I)
   53 CONTINUE
      NITE=NITE+1
      IF(MNO.EQ.NSTART.OR.MNO.EQ.(NDIV+1))GO TO 161
      DO 162 I=2,M-1
      C(I)=XU(I)*XLE+XV(I)*CC(I)+DD(I)*XNU(I)
  162 E(I)=XU(I)*(U(2,I)*XLC-U(1,I)*XLD)-1./RHO(I)*DPRES
      GO TO 164
  161 DO 163 I=2,M-1
      C(I)=XU(I)/DXM1+XV(I)*CC(I)+DD(I)*XNU(I)
  163 E(I)=XU(I)*U(2,I)/DXM1-1./RHO(I)*DPRESA
  164 CONTINUE
      E(M-1)=E(M-1)-B(M-1)*UINF(MNO)
      E(2)=E(2)-D(2)*UU(1)
      DO 58 I=1,M-2
      E(I)=E(I+1)
   58 A(I,I)=C(I+1)
      DO 59 I=1,M-3
   59 A(I,I+1)=B(I+1)
      DO 60 I=2,M-2
   60 A(I,I-1)=D(I+1)
      ML=M-2
      CALL GAUSS(A,UUU,E,ML)
      DO 62 I=2,M-1
   62 UU(I)=UUU(I-1)
      UU(1)=UW
      IF(MNO.EQ.NSTART.OR.MNO.EQ.(NDIV+1))GO TO 165
      DO 65 I=2,M-1
      VV(I)=1./RHO(I)*(VV(I-1)*RHO(I-1)-DYM1(I)/2.*((U(1,I)*
     $RHO1(I)+U(1,I-1)*RHO1(I-1))*XLD-(U(2,I)*RHO2(I)+U(2,I-1)
     $*RHO2(I-1))*XLC+(UU(I)*RHO(I)+UU(I-1)*RHO(I-1))*XLE))
   65 XW(I)=VV(I)
      GO TO 166
  165 DO 167 I=2,M-1
      VV(I)=1./RHO(I)*(VV(I-1)*RHO(I-1)-DYM1(I)/2.*(UU(I)*RHO(I)
     $+UU(I-1)*RHO(I-1)-U(2,I)*RHO2(I)-U(2,I-1)*RHO2(I-1))/DXM1)
  167 XW(I)=VV(I)
  166 CONTINUE
      IF(ICOMP.EQ.0)GO TO 908
  910 CONTINUE
      UU(M)=UINF(MNO)
      DO 201 I=2,M-1
      VV(I)=VV(I)-1./RE/RHO(I)*(XMU(I+1)*AA(I)/PRNO(I+1)
     $-XMU(I-1)*FE(I)/PRNO(I-1)+XMU(I)*CC(I)/PRNO(I))
      B(I)=VV(I)*AA(I)-BB(I)*XNU(I)/PRNO(I)
      VISDIS(I)=ECK*(UU(I+1)*AA(I)-UU(I-1)*EE(I)+UU(I)
     $*CC(I))**2*XNU(I)
  201 D(I)=-VV(I)*FE(I)-FG(I)*XNU(I)/PRNO(I)
      IF(MNO.EQ.NSTART.OR.MNO.EQ.(NDIV+1))GO TO 202
      DO 203 I=2,M-1
      C(I)=UU(I)*XLE+VV(I)*CC(I)+DD(I)*XNU(I)/PRNO(I)
  203 E(I)=UU(I)*(T(2,I)*XLC-T(1,I)*XLD)+VISDIS(I)
     $+ECK*UU(I)/RHO(I)*DPRES
      GO TO 204
  202 DO 205 I=2,M-1
      C(I)=UU(I)/DXM1+VV(I)*CC(I)+DD(I)*XNU(I)/PRNO(I)
  205 E(I)=UU(I)*T(2,I)/DXM1+VISDIS(I)+ECK*UU(I)/RHO(I)*DPRESA
  204 CONTINUE
      E(M-1)=E(M-1)-B(M-1)*TINF(MNO)
      IF(MNO.LT.NSTART.OR.MNO.GT.NDIV)B(2)=B(2)-D(2)/SL
     $/(2.+SL)
      IF(MNO.LT.NSTART.OR.MNO.GT.NDIV)C(2)=C(2)+D(2)/SL
     $/(2.+SL)*(1.+SL)**2
```

```
      DO 331 I=1,M-2
      E(I)=E(I+1)
  331 A(I,I)=C(I+1)
      DO 332 I=1,M-3
  332 A(I,I+1)=B(I+1)
      DO 333 I=2,M-2
  333 A(I,I-1)=D(I+1)
      CALL GAUSS(A,TTT,E,ML)
      DO 209 I=2,M-1
  209 TT(I)=TTT(I-1)
      TWALL=(1.+SL)**2/SL/(2.+SL)*TT(2)-TT(3)/SL/(2.+SL)
      IF(MNO.GE.NSTART.AND.MNO.LE.NDIV)TWALL=0.
      XT(1)=TWALL
      XT(M)=TINF(MNO)
      IF(ICOMP.EQ.0)GO TO 911
  908 DO 66 I=2,M-1
      IF(ABS(1.-UU(I)/XU(I)).LT.EPS)GO TO 66
      DO 68 J=2,M-1
      XU(J)=UU(J)
      XT(J)=TT(J)
   68 XV(J)=XW(J)
      GO TO 52
   66 CONTINUE
      IF(ICOMP.EQ.0)GO TO 910
  911 CONTINUE
      XW(1)=VV(1)
      TT(1)=TWALL
      DO 528 I=1,M-1
      TTE(I)=TT(I)/TINF(MNO)
      UUE(I)=UU(I)/UINF(MNO)
  528 VVE(I)=XW(I)/UINF(MNO)
      DTDIF=(XT(2)-TT(2))/XT(2)
      WRITE(6,120)MNO
  120 FORMAT(//,20X,'******STATION  NO.=    ',I7,///)
  110 FORMAT(//,10X,'DIMENSIONLESS Y-COORD.S',//)
      WRITE(6,119)XX(3),U(1,1),U(2,1),UU(1),VV(1),T(1,1)
     $,T(2,1),TWALL,NITE,UINF(MNO),TINF(MNO)
  119 FORMAT(//,5X,'XX(3)=',F7.5,1X,'U(1,1)=',F6.5,1X,'U(2,1)='
     $,F6.5,1X,'UU(1)=',F6.5,1X,'VV(1)=',F6.5,//,5X,'T(1,1)='
     $,F8.6,1X,'T(2,1)=',F8.6,1X,'TWALL=',F8.6,1X,'NITE=',I3
     $,1X,'UE=',F8.6,2X,'TE=',F8.6,//)
      IF(JPRINT.EQ.0)GO TO 657
      PRINT*,'   '
      PRINT*,'              TANGENTIAL COMPONENT OF VELOCITY (U/UE)
      WRITE(6,71)(I,UUE(I),I=1,M-1)
      PRINT*,'  '
      PRINT*,'              NORMAL COMPONENT OF VELOCITY  (V/UE) '
      WRITE(6,71)(I,VVE(I),I=1,M-1)
      PRINT*,'  '
      PRINT*,'              TEMPERATURE PROFILE   (T-TC)/(TE-TC)
      WRITE(6,71)(I,TTE(I),I=1,M-1)
  657 EFFECT=1.-TWALL/(1.+ECK/2.)
      XOO=XST+2.*DXP
      FRIC=SQRT(XOO*XMU(1)/RHO(1)/RE)*(UU(2)*(1.+1./SL)-UU(3)/S
     $/(1.+SL)-UU(1)*(SL+2.)/(1.+SL))/DY
      PRINT*,'   '
      PRINT*,'EFFECTIVENESS',EFFECT,'FRIC= ',FRIC
      PRINT*,'   '
      PRINT*,'(XT(2)-TT(2))/XT(2)=',DTDIF
   71 FORMAT(7(1X,I2,F10.6))
      TT(1)=TWALL
      XW(1)=VV(1)
      U(2,M)=UINF(MNM)
      T(2,M)=TINF(MNM)
      TT(M)=TINF(MNO)
      IF(MNO.EQ.IFILE)WRITE(Tw,514)M,(U(2,I),UU(I),T(2,I)
     $,TT(I),XW(I),I=1,M)
      XX(1)=XX(2)
      XX(2)=XX(3)
      DO 69 I=2,M-1
      RHO1(I)=RHO2(I)
      RHO2(I)=RHO(I)
      T(1,I)=T(2,I)
      T(2,I)=TT(I)
      U(1,I)=U(2,I)
      V(1,I)=V(2,I)
      V(2,I)=XW(I)
   69 U(2,I)=UU(I)
      IF(MNO.EQ.(NSTART-1))DX=DXSL
      IF(MNO.GE.NSTEP)DX=1.05*DX
      IF(MNO.EQ.NSTEP1)DX=DXP
      XX(3)=XX(3)+DX
      MNO=MNO+1
```

```
      ISTN=ISTN+1
      XX3=XX(3)
      IF(IFLAT.EQ.1)GO TO 665
      UINF(MNO)=AITINT(XSURF,UF1,NMAX,XX3,K,P)
      TINF(MNO)=1.+ECK*(1.-UINF(MNO)**2)/2.
      PRES(MNO)=((1.-TINF(MNO))*TRATIO+TINF(MNO))**3.5
      GO TO 666
 665  UINF(MNO)=1.
      TINF(MNO)=1.
      PRES(MNO)=1.
 666  T(1,1)=T(2,1)
      IF((MNO-1).GE.NSTART.AND.(MNO-2).LT.NDIV)T(1,1)=0.
      T(2,1)=TWALL
      IF(MNO.GE.NSTART.AND.(MNO-1).LT.NDIV)T(2,1)=0.
      IF(MNO.EQ.(NDIV+1))T(2,1)=(1.+SL)**2/SL/(2.+SL)*TT(2)
     $-TT(3)/SL/(2.+SL)
      IF(ICOMP.EQ.0)GO TO 912
      RHO1(1)=PRES(MNO-2)/(T(1,1)+(1.-T(1,1))*TRATIO)
      RHO2(1)=PRES(MNO-1)/(T(2,1)+(1.-T(2,1))*TRATIO)
      GO TO 913
 912  RHO1(1)=1.
      RHO2(1)=1.
 913  CONTINUE
      NITE=0.
      IF(ISTN.GT.NSTOP)GO TO 70
      IF(M.GT.MMAX)GO TO 646
      GO TO 51
 646  PRINT*,'******MMAX  REACHED******'
  70  STOP
      END
      SUBROUTINE GAUSS(A,X,B,N)
      DIMENSION A(90,90),X(90),B(90)
      DOUBLE  PRECISION  A,X,B
      DO 5 I=2,N
      RATIO=A(I,I-1)/A(I-1,I-1)
      A(I,I)=A(I,I)-A(I-1,I)*RATIO
   5  B(I)=B(I)-B(I-1)*RATIO
      X(N)=B(N)/A(N,N)
      DO 6 I=1,N-1
      J=N-I
   6  X(J)=(B(J)-A(J,J+1)*X(J+1))/A(J,J)
      RETURN
      END
```

Sample Input/Output

The computer program necessitates two upstream tangential velocity and temperature profiles, which are obtained from Cebeci's program(22). Outer edge velocity distribution is obtained from Katsanis' program(23). The disk unit number where the data obtained from these programs are recorded are as follows:

D a t a	Disk Unit No
Blade surface coordinates at nodal points (ft)	8
Outer edge velocity distribution (ft/sec)	10
Nodal values of normal coordinate and velocity at the first station, (ft, ft/sec)	12
Nodal values of normal coordinate and velocity at the second station	13
Temperature distribution at the first station (^{o}R)	14
Temperature distribution at the second station	15

Fig.29, shows the finite difference mesh structure used to prepare input data to the computer program.

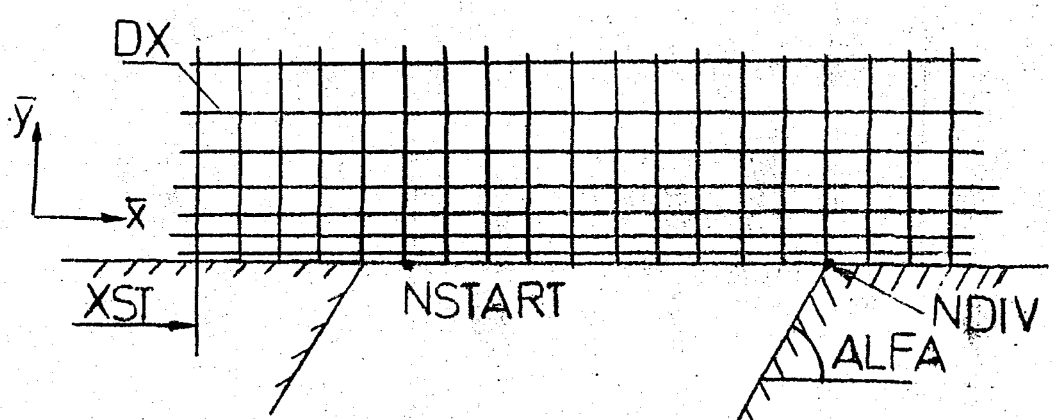

Fig.29- Finite-difference mesh structure

The following is the description of input data:

ICOMP	1: Compressible 0: Incompressible
IFLAT	1: Zero-pressure gradient-flat plate 0: Flow over the blade
ICONT	1: Initial velocity and temperature profiles are taken from the previous run 0: Initial velocity and temperature profiles are taken from Cebeci's program(22)
JPRINT	1: Velocity and temperature profiles at each station as well as station data are printed out 0: Only station data (e.g., streamwise coordinate, effectiveness, outer edge values) are printed out
IFILE	Station number where velocity and temperature profiles are written down on disk for the next use (See ICONT)
IR	Disk unit number where velocity and temperature profiles have been recorded
IW	Disk unit number where velocity and temperature profiles to be recorded for further use
MSTART	Number of nodal points in normal direction for initial stations
MJ	Station number where boundary layer thickness check is stopped
NSTART	Station number where injection begins
NDIV	Trailing edge station number
NSTEP	Station number where streamwise step size is increased
NSTEP1	Station number from which on Δx is increased gradually

NSTOP	Station number where execution is stopped
M	Maximum number of nodal points in normal direction
NMAX	Number of nodal points along the blade surface
NNMAX	Number of nodal points in normal direction in Cebeci's program(22)
XST	Dimensionless streamwise coordinate of the first initial station
ALFA	Injection angle (deg.)
CHORD	Characteristic length (Chord)(ft)
DXSL	Streamwise step size over the slot
SL	Magnification factor, k
YMAX	Maximum dimensionless normal Coordinate
DX	Dimensionless step size in streamwise direction
MRATIO	Blowing rate parameter or injection ratio defined as $(\rho_c v_c)/\rho_o U_o$ (comp.) or v_c/U_o (incomp.)
UD	Reference free stream velocity (ft/s)
RE	Reference Reynolds number $Re = \frac{\rho_o U_o c}{\mu_o}$
TTO	Free stream static temperature (^oK)
TCOOL	Coolant temperature (^oK)

Input formats and a sample input/output for the mesh structure (Fig.29) for the compressible flow over the blade are as follows:

Variable	Format
ICOMP, IFLAT, ICONT, JPRINT, IFILE, IR, IW, MSTART, MJ, NSTART, NDIV, NSTEP, NSTEP1, NSTOP, M, NMAX, NNMAX	4I1,13I3
XST, ALFA, CHORD, DXSL, YMAX, DX	7F10.0
MRATIO, UO, RE, TTO, TCOOL	5F10.0
EETA(I), DDF(I)	3(2F10.0)

M= 72 NDTV= 18 NSTART= 4 MJ= 19 NNMAY= 32

NMAX= 51 NSTEP= 28 NSTOP=100 ICONT= 0 IFILE=200 MSTART= 55

SL=1.05 EPS= .000500 YMAX= .0618950 RE= 70248.000

ECK= .01632051 UC=328.084 CHORD= .401250 PRESO= 38.98737

TCOOL=750.00 TTC= 1357.1370 XST= .19500 DXSL= .00100

MRATIO= .0250 ALFA= 84.00

DIMENSIONLESS Y-COORD.S

1	.000000	2	.000100	3	.000205	4	.000315	5	.000431	6	.000553	7	.000680
8	.000814	9	.000955	10	.001103	11	.001258	12	.001421	13	.001592	14	.001771
15	.001960	16	.002158	17	.002366	18	.002584	19	.002813	20	.003054	21	.003307
22	.003572	23	.003850	24	.004143	25	.004450	26	.004773	27	.005111	28	.005467
29	.005840	30	.006232	31	.006644	32	.007076	33	.007530	34	.008006	35	.008507
36	.009032	37	.009584	38	.010163	39	.010771	40	.011409	41	.012080	42	.012784
43	.013523	44	.014299	45	.015114	46	.015970	47	.016868	48	.017812	49	.018802
50	.019843	51	.020935	52	.022081	53	.023285	54	.024550	55	.025877	56	.027271
57	.028735	58	.030271	59	.031885	60	.033579	61	.035358	62	.037226	63	.039187
64	.041247	65	.043409	66	.045679	67	.048063	68	.050567	69	.053195	70	.055955
71	.058852	72	.061895										

DIM.LESS OUTER EDGE TEMP.

1	1.005017	2	1.004988	3	1.004963	4	1.004865	5	1.004756	6	1.004691	7	1.004652
8	1.004541	9	1.004349	10	1.004103	11	1.003828	12	1.003523	13	1.003219	14	1.002910
15	1.002691	16	1.002509	17	1.002381	18	1.002235	19	1.002090	20	1.001887	21	1.001671
22	1.001258	23	1.000763	24	1.000174	25	.999496	26	.998741	27	.997909	28	.997008
29	.996071	30	.995085	31	.994030	32	.992897	33	.991661	34	.990329	35	.988860
36	.987220	37	.985453	38	.983598	39	.981644	40	.979700	41	.977788	42	.975928
43	.974315	44	.972853	45	.971512	46	.970319	47	.969172	48	.967959	49	.964941
50	.862084	51	1.008160										

NORMALIZED PRES. GRADIENT

1	1.007877	2	1.007832	3	1.007793	4	1.007639	5	1.007467	6	1.007365	7	1.007304
8	1.007129	9	1.006826	10	1.006439	11	1.006006	12	1.005526	13	1.005049	14	1.004564
15	1.004204	16	1.003932	17	1.003733	18	1.003504	19	1.003276	20	1.002958	21	1.002556
22	1.001971	23	1.001195	24	1.000273	25	.999212	26	.998030	27	.996728	28	.995324
29	.993862	30	.992326	31	.990683	32	.988915	33	.987003	34	.984940	35	.982666
36	.980132	37	.977408	38	.974537	39	.971552	40	.968574	41	.965650	42	.962813
43	.960357	44	.958134	45	.956100	46	.954292	47	.952556	48	.950727	49	.946172
50	.800199	51	1.012836										

SURFACE COORD.S (FT.)

1	.000000	2	.009939	3	.018516	4	.027018	5	.035524	6	.044065	7	.052675
8	.061392	9	.070247	10	.079235	11	.088342	12	.097550	13	.106839	14	.116187
15	.125570	16	.134986	17	.144466	18	.154042	19	.163750	20	.173628	21	.183719
22	.194066	23	.204684	24	.215562	25	.226686	26	.238079	27	.249600	28	.261351
29	.273272	30	.285363	31	.297633	32	.310095	33	.322758	34	.335633	35	.348732
36	.362062	37	.375607	38	.389343	39	.403247	40	.417294	41	.431459	42	.445717
43	.460050	44	.474462	45	.488962	46	.503558	47	.518259	48	.533073	49	.548007
50	.563072	51	.571173										

DIM.LESS OUTER EDGE VEL.

1	.620653	2	.623489	3	.625936	4	.635426	5	.645852	6	.652019	7	.655642
8	.665957	9	.683397	10	.705152	11	.728636	12	.753871	13	.778154	14	.802134
15	.819426	16	.832268	17	.841572	18	.852129	19	.862489	20	.876793	21	.894499
22	.919689	23	.952091	24	.989260	25	1.030398	26	1.074396	27	1.120873	28	1.169021
29	1.217155	30	1.265808	31	1.315904	32	1.367845	33	1.421953	34	1.478203	35	1.537896
36	1.601906	37	1.668124	38	1.735295	39	1.802633	40	1.867521	41	1.929248	42	1.987444
43	2.036562	44	2.080094	45	2.119222	46	2.153434	47	2.185838	48	2.219570	49	2.301393
50	4.230946	51	.000000										

NITIAL VELOCITY PROFILE (U/UO) STATION NO.= 1

1	.000000	2	.021313	3	.047157	4	.065506	5	.088334	6	.111610	7	.135300
8	.159369	9	.183779	10	.208491	11	.233467	12	.258652	13	.284015	14	.309502
15	.335064	16	.360644	17	.386178	18	.411592	19	.436802	20	.461706	21	.486195
22	.510101	23	.533297	24	.555594	25	.576802	26	.596718	27	.615142	28	.631889
29	.646799	30	.659760	31	.670718	32	.679694	33	.686783	34	.692157	35	.696046
36	.698718	37	.700450	38	.701503	39	.702097	40	.702410	41	.702560	42	.702627
43	.702650	44	.702652	45	.702651	46	.702660	47	.702661	48	.702661	49	.702661
50	.702661	51	.702661	52	.702661	53	.702661	54	.702661	55	.702661		

INITIAL TEMPERATURE PROFILE (T-TC)/(TO-TC)

1	1.007585	2	1.007582	3	1.007573	4	1.007559	5	1.007538	6	1.007510	7	1.007476
8	1.007433	9	1.007383	10	1.007324	11	1.007258	12	1.007183	13	1.007099	14	1.007007
15	1.006906	16	1.006796	17	1.006678	18	1.006552	19	1.006418	20	1.006277	21	1.006129
22	1.005976	23	1.005819	24	1.005659	25	1.005498	26	1.005338	27	1.005181	28	1.005030
29	1.004887	30	1.004755	31	1.004635	32	1.004529	33	1.004439	34	1.004364	35	1.004303
36	1.004257	37	1.004223	38	1.004199	39	1.004183	40	1.004173	41	1.004167	42	1.004164
43	1.004162	44	1.004162	45	1.004162	46	1.004162	47	1.004131	48	1.004131	49	1.004131
50	1.004131	51	1.004131	52	1.004131	53	1.004131	54	1.004131	55	1.004131		

NITIAL VELOCITY PROFILE (U/UO) STATION NO.= 2

1	.000000	2	.021562	3	.043662	4	.066274	5	.089369	6	.112913	7	.136871
8	.161202	9	.185865	10	.210816	11	.236010	12	.261399	13	.286936	14	.312571
15	.338250	16	.363918	17	.389509	18	.414952	19	.440162	20	.465041	21	.489474
22	.513326	23	.536443	24	.558652	25	.579766	26	.599588	27	.617922	28	.634586
29	.649425	30	.662327	31	.673242	32	.682188	33	.689262	34	.694632	35	.698525
36	.701204	37	.702945	38	.704006	39	.704607	40	.704924	41	.705077	42	.705146
43	.705170	44	.705172	45	.705172	46	.705181	47	.705181	48	.705181	49	.705181
50	.705181	51	.705181	52	.705181	53	.705181	54	.705181	55	.705181		

INITTIAL TEMPFRATURE PROFILE (T-TC)/(TO-TC)

1	1.007580	2	1.007578	3	1.007569	4	1.007554	5	1.007533	6	1.007504	7	1.007469
8	1.007425	9	1.007374	10	1.007314	11	1.007246	12	1.007170	13	1.007084	14	1.006990
15	1.006888	16	1.006777	17	1.006657	18	1.006530	19	1.006395	20	1.006252	21	1.006104
22	1.005950	23	1.005792	24	1.005632	25	1.005470	26	1.005310	27	1.005153	28	1.005002
29	1.004860	30	1.004727	31	1.004607	32	1.004502	33	1.004411	34	1.004336	35	1.004275
36	1.004229	37	1.004194	38	1.004170	39	1.004154	40	1.004144	41	1.004138	42	1.004135
43	1.004133	44	1.004132	45	1.004132	46	1.004132	47	1.004102	48	1.004102	49	1.004102
50	1.004102	51	1.004102	52	1.004102	53	1.004102	54	1.004102	55	1.004102		

******STATION NO.= 3

XX(3)= .20000 U(1,1)=.00000 U(2,1)=.00000 UU(1)=.00000 VV(1)=.00000

T(1,1)=1.007585 T(2,1)=1.007580 TWALL=1.007575 NITE= 4 UE= .707715 TE=1.004073

TANGENTIAL COMPONENT OF VELOCITY (U/UE)

1	.000000	2	.030763	3	.062298	4	.094568	5	.127530	6	.161134	7	.195327
8	.230047	9	.265230	10	.300809	11	.336713	12	.372869	13	.409205	14	.445644
15	.482109	16	.518515	17	.554773	18	.590780	19	.626420	20	.661558	21	.696034
22	.729663	23	.762235	24	.793510	25	.823232	26	.851127	27	.876926	28	.900376
29	.921261	30	.939429	31	.954807	32	.967424	33	.977411	34	.985002	35	.990514
36	.994316	37	.996792	38	.998305	39	.999165	40	.999620	41	.999841	42	.999939
43	.999974	44	.999979	45	.999979	46	.999991	47	.999991	48	.999991	49	.999991
50	.999991	51	.999991	52	.999991	53	.999991	54	.999991				

NORMAL COMPONENT OF VELOCITY (V/UE)

1	.000000	2	-.000005	3	-.000022	4	-.000053	5	-.000099	6	-.000162	7	-.000244
8	-.000348	9	-.000475	10	-.000627	11	-.000806	12	-.001013	13	-.001248	14	-.001513
15	-.001805	16	-.002125	17	-.002472	18	-.002843	19	-.003237	20	-.003652	21	-.004084
22	-.004533	23	-.004996	24	-.005471	25	-.005957	26	-.006455	27	-.006964	28	-.007485
29	-.008020	30	-.008572	31	-.009145	32	-.009741	33	-.010366	34	-.011022	35	-.011714
36	-.012444	37	-.013215	38	-.014028	39	-.014885	40	-.015787	41	-.016736	42	-.017733
43	-.018780	44	-.019880	45	-.021036	46	-.022249	47	-.023522	48	-.024860	49	-.026264
50	-.027738	51	-.029286	52	-.030912	53	-.032619	54	-.034411				

TEMPERATURE PROFILE (T-TC)/(TE-TC)

1	1.003498	2	1.003485	3	1.003477	4	1.003462	5	1.003440	6	1.003411	7	1.003375
8	1.003331	9	1.003279	10	1.003218	11	1.003149	12	1.003071	13	1.002985	14	1.002890
15	1.002786	16	1.002674	17	1.002554	18	1.002425	19	1.002290	20	1.002147	21	1.001998
22	1.001844	23	1.001686	24	1.001526	25	1.001365	26	1.001205	27	1.001049	28	1.000898
29	1.000756	30	1.000624	31	1.000505	32	1.000399	33	1.000309	34	1.000234	35	1.000173
36	1.000127	37	1.000092	38	1.000068	39	1.000052	40	1.000042	41	1.000036	42	1.000032
43	1.000031	44	1.000030	45	1.000030	46	1.000028	47	1.000001	48	1.000000	49	1.000000
50	1.000000	51	1.000000	52	1.000000	53	1.000000	54	1.000000				

EFFECTIVENESS .58040023-003 FRIC= .37141730

(XT(2)-TT(2))/XT(2)= -.22183761-006